

Internal Note No. 68-FM-310



NATIONAL AERONAUTICS AND SPACE ADMINISTRATION

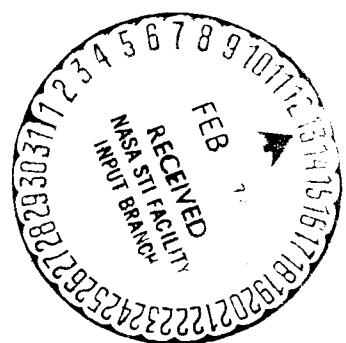
MSC INTERNAL NOTE NO. 68-FM-310

December 30, 1968

Technical Library, Bellcomm, Inc.

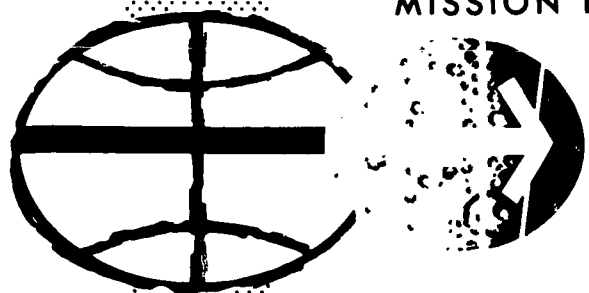
Nov 1968

PARKING ORBITS ALINED USING
PLANETARY OBLATENESS FOR DIRECT
MARS MISSIONS BETWEEN 1975
AND 1988



Advanced Mission Design Branch

MISSION PLANNING AND ANALYSIS DIVISION



MANNED SPACECRAFT CENTER
HOUSTON, TEXAS

(NASA-TM-X-69761) PARKING ORBITS ALINED
USING PLANETARY OBLATENESS FOR DIRECT
MARS MISSIONS BETWEEN 1975 AND 1988
(NASA) 70 p

N74-70720

Unclas

00/99 16428

MSC INTERNAL NOTE NO. 68-FM-310

PARKING ORBITS ALINED USING PLANETARY OBLATENESS
FOR DIRECT MARS MISSIONS BETWEEN 1975 AND 1988

By Joseph R. Thibodeau III and Gregory A. Zambo
Advanced Mission Design Branch

December 30, 1968


MISSION PLANNING AND ANALYSIS DIVISION
NATIONAL AERONAUTICS AND SPACE ADMINISTRATION
MANNED SPACECRAFT CENTER
HOUSTON, TEXAS

Approved:


Jack Funk, Chief

Advanced Mission Design Branch

Approved:


John P. Mayer, Chief

Mission Planning and Analysis Division

CONTENTS

Section	Page
SUMMARY	1
INTRODUCTION	2
ANALYSIS	5
Scanning Mars Orbital Missions Between 1975 and 1988 . . .	6
The minimum ΔV missions	6
How Oblateness Affects the Parking Orbit Selection	7
RESULTS	8
Parking Orbits Available During Conjunction Class Missions	9
Parking Orbits Available During Opposition Class Missions	10
The Effect of Stay Time on the Parking Orbit	11
The Correlation of Eccentricity and Inclination	12
CONCLUDING REMARKS	14
REFERENCES	63

TABLES

Table		Page
I	EARTH-ORBITAL LAUNCH DATES AND TRIP TIMES FOR MINIMUM ΔV MISSIONS TO MARS	16
II	EARTH-ORBITAL LAUNCH DATES AND TRIP TIMES FOR SHORT STAY TIME MISSIONS TO MARS	17
III	SUMMARY OF MARS PARKING ORBITS WHICH OCCURRED DURING THE CONJUNCTION CLASS MISSIONS	
	(a) Earth departure date, August 25, 1975	18
	(b) Earth departure date, October 13, 1977	18
	(c) Earth departure date, October 26, 1979	18
	(d) Earth departure date, November 21, 1981	18
	(e) Earth departure date, December 21, 1983	19
	(f) Earth departure date, May 4, 1986	19
	(g) Earth departure date, July 10, 1988	19
IV	SUMMARY OF MARS PARKING ORBITS WHICH OCCURRED DURING THE OPPOSITION CLASS MISSIONS	
	(a) Earth departure date, September 14, 1975	20
	(b) Earth departure date, November 2, 1977	20
	(c) Earth departure date, November 22, 1979	20
	(d) Earth departure date, November 11, 1981	20
	(e) Earth departure date, December 31, 1981	20
	(f) Earth departure date, December 21, 1983	20
	(g) Earth departure date, February 29, 1984	21
	(h) Earth departure date, April 19, 1986	21
	(i) Earth departure date, June 27, 1988	21
V	THE NUMBER AND SELECTION OF PARKING ORBITS AND THEIR DEPENDENCE ON THE ORBITAL STAY DURING THE 1986 OPPOSITION CLASS MISSION	22
VI	SUMMARY OF REGRESSING PARKING ORBITS WHICH SHIFT INTO ALINEMENT DURING THE 1977 CONJUNCTION CLASS MISSION	
	(a) Launch date from earth parking orbit, September 23, 1977	23
	(b) Launch date from earth parking orbit, October 13, 1977	23
	(c) Launch date from earth parking orbit, November 12, 1977	24

VII SUMMARY OF REGRESSING PARKING ORBITS WHICH SHIFT
INTO ALINEMENT DURING THE 1986 OPPOSITION
CLASS MISSION

(a)	Launch date from earth parking orbit, April 19, 1986	25
(b)	Launch date from earth parking orbit, April 29, 1986	25
(c)	Launch date from earth parking orbit, May 9, 1986	25

FIGURES

Figure		Page
1	Heliocentric schematic illustrating the conjunction class mission and the parking orbit about Mars . . .	26
2	Heliocentric schematic illustrating the opposition class mission and the parking orbit about Mars . . .	27
3	The variation of mission velocity requirements for minimum ΔV missions	
	(a) The 1975 mission window	28
	(b) The 1977 mission window	29
	(c) The 1979 mission window	30
	(d) The 1981 mission window	31
	(e) The 1983 mission window	32
	(f) The 1986 mission window	33
	(g) The 1988 mission window	34
4	Variation of mission velocity requirements during the Earth-orbital alunch window for minimum ΔV Mars orbital missions between 1975 and 1990	35
5	Variation of mission velocity requirements during the Earth-orbital launch window for short stay time Mars orbital missions between 1975 and 1990	36
6	The variation of mission velocity requirements for the short stay time missions	
	(a) 1981 mission window	37
	(b) 1983 and 1984 mission windows	38
7	Variation of trip times during the mission launch window for the minimum ΔV Mars orbital missions between 1975 and 1988	39
8	Launch dates and trip times for short stay time missions between 1975 and 1988	40
9	The perihelion distance of the return trajectory for short stay time missions between 1975 and 1988	41

Figure		Page
10	The orbital elements of the parking orbits for minimum ΔV missions	
	(a) The 1975 mission window	42
	(b) The 1977 mission window	43
	(c) The 1979 mission window	44
	(d) The 1981 mission window	45
	(e) The 1983 mission window	46
	(f) The 1986 mission window	47
	(g) The 1988 mission window	48
11	The range of apoapsis altitudes and orbital inclinations which occur during the minimum ΔV missions between 1975 and 1988	49
12	The orbital elements of the parking orbit for the short stay time missions	
	(a) The 1975 mission window	50
	(b) The 1977 mission window	51
	(c) The 1979 mission window	52
	(d) The 1981 mission window	53
	(e) The 1983 mission window	54
	(f) The 1984 mission window	55
	(g) The 1986 mission window	56
	(h) The 1988 mission window	57
13	The range of apoapsis altitudes and orbital inclinations which occur during short stay time missions between 1975 and 1988	58
14	Variation of orbital eccentricity with stay time for a stational V_{∞} geometry	59
15	Secular rotation rates of the parking orbit node and periapsis position vectors due to planetary oblateness	60
16	The correlation of apoapsis altitude and orbital inclination for regressing orbits which occur during a minimum ΔV mission in 1977	61
17	The correlation of apoapsis altitude and orbital inclination for the short stay time mission in 1986	62

PARKING ORBITS ALINED USING PLANETARY OBLATENESS

FOR DIRECT MARS MISSIONS BETWEEN 1975 AND 1988

By Joseph R. Thibodeau III and Gregory A. Zambo

SUMMARY

A study was made of the feasibility of using the oblateness of the planetary gravitational field to aline the parking orbit during direct, round-trip capture missions to Mars between 1975 and 1988. An analytical technique was used to define the possible configurations of elliptical parking orbits which shift into alinement for departure and require no discrete propulsive maneuvers. Parking orbits were found for the minimum total ΔV members of both the conjunction and the opposition classes of Mars missions.

Results indicate that moderate to highly elliptic parking orbits (eccentricity from 0.4 to 0.8) can be used at Mars for both classes of missions, and both the planetary arrival and departure maneuvers will occur at periapsis. The inclinations commonly occur in narrow bands which are widely distributed over the range from 0° to 180° . The highest eccentricity orbits have low inclinations and may be either posigrade or retrograde with respect to the planetary axis of rotation.

INTRODUCTION

Contemplating the possibility of manned expeditions to the near planets, one often considers the problem: What kind of parking orbit is best suited for a manned orbital mission? A moment's reflection reveals this question is nearly impossible to answer. Ultimately, the design of the parking orbit must depend on limitations imposed by the hardware, the mission objectives, and the physical laws of nature, and, like the mission itself, can only be determined by intensive study of many design elements.

Some insight into the problem can be gained by studying the behavior of the parking orbit and the resultant operational requirements imposed by various configurations of the parking orbit. This paper takes a much narrower view of this problem by studying the behavior of parking orbits constrained to the motion which results from the oblateness of the planet's gravitational field. These parking orbits can be referred to loosely as the elliptical regressing parking orbit. They require no discrete propulsive maneuvers for orbital alinement.^a These maneuvers are here defined to be either discrete or combined with the planetary capture and escape maneuvers.

Of course, the idea of using planetary oblateness for parking orbit alinement is not new. There are various allusions to it in the literature. The remarks are often connected with other considerations in trajectory design. A discussion of the technique of using oblateness for orbit alinement is presented in references 1, 2, 3, and 4.

The authors feel these orbits, as a group, exhibit many interesting properties which make them worthy of study on their own merits; therefore, a detailed study of their behavior and characteristics was undertaken. This report documents the results of this study.

The main contribution of the paper is to indicate the feasibility of using oblateness for parking orbit alinement, the implications of this technique, its limitations, and its flexibility for application during preliminary analysis of orbital missions to Mars.

Basically, the use of planetary oblateness for orbital alinement implies the selection of the orbital elements of the parking orbit so that the resulting nodal and apsidal motion will shift the orbit into

^aExcept perhaps those required to correct guidance and navigational uncertainties. (Consideration of these problems would be required during the course of any operational trajectory and are beyond the scope of this paper.)

proper alinement for departure on the intended date. Employing this type of orbit allows the use of coplanar periapsis impulses for both the orbital capture and escape maneuvers. In many cases, although not always, ΔV costs may be reduced because highly elliptic orbits can be used at the target planet and because the orbital capture and escape maneuvers are coplanar, thereby reducing or eliminating the need of plane changes and flight-path angle corrections. This type of orbit represents an excellent point of departure for further study of parking orbits which may require a combination of perturbations and corrective propulsive maneuvers for orbital alinement to achieve both the lowest possible total mission ΔV and the best trade-off between other mission design criteria.

In order to establish norms for the behavior of the parking orbit, the orbital missions to Mars were examined for each Earth orbital launch opportunity from 1975 to 1988. The primary emphasis was to find out how many different elliptical orbits are available and what are the characteristics of the ones that exhibit the highest eccentricities. Also of interest was the effect of the Earth orbital launch window and resultant variations of the geometry of planetary approach and departure. The emphasis of this investigation was to find out if the parking orbits exhibit smooth variations in characteristics and if they are available over a wide range of both the stay-time and the geometry of approach and departure.

If this approach allows the use of highly eccentric orbits without the need of auxiliary propulsive maneuvers, this fact can have a fundamental impact on the design of orbital missions for which small excursion vehicles can be used for close orbital reconnaissance or landing on the surface of the planet.

The command spacecraft of an interplanetary expedition is large and must therefore be considered as a space station or platform which serves as a base from which small excursion vehicles are used to complete mission objectives. There is a definite possibility that the command spacecraft could be placed in an elliptical parking orbit of the type investigated in this report. A small excursion vehicle could then be separated from the command spacecraft, establish a different orbit consistent with the mission objectives and crew safety, and return to the command spacecraft.

This is the main reason why this study was undertaken. Of course, much work is needed to determine the feasibility of this approach.

Design of the parking orbit is, of course, meaningful only in the context of complete mission profiles. The missions must be defined before the parking orbit can be studied. For this study, the direct, round-trip Mars capture missions were investigated and the minimum ΔV

trajectories associated with both opposition and conjunction classes of Mars missions were selected. These two classes of missions are probably indicative of both the best and the worst possible cases where oblateness could conceivably be used for orbital alinement, mostly because the opposition class missions have very short stay-times, from 10 to 40 days, and because the conjunction class missions have very long stay-times, from 300 to 500 days. (These missions are referred to later as simply the "long" or "short" missions. The long missions are sometimes called minimum ΔV because the heliocentric trajectories are the two-impulse, absolute minimum ΔV , or near-Hohmann transfers. The short missions exhibit only local minimums in total mission ΔV when certain of the trajectory parameters are constrained (i.e., the flight times or earth entry velocity).

The heliocentric trajectories, launch dates, and trip times were selected to yield missions with the lowest possible total mission ΔV requirements. The process of mission selection was done automatically by a mission scanning program developed by Mr. E. W. Henry of the Advanced Mission Design Branch. The authors wish to thank Mr. Henry for the data supplied by this program.

ANALYSIS

Orbital missions to Mars were examined for each Earth orbital launch opportunity from 1975 to 1988. The analysis of these missions was performed in two steps. The first step was simply to find the missions and define the characteristics of the heliocentric trajectories, the launch dates, and the flight times. Both the opposition and conjunction classes of missions were found. This phase of the analysis was greatly facilitated by an automatic mission scanning program which produced the launch dates and flight times for these missions. This program, documented in reference 4, produced optimum launch dates and flight times for these missions based on the selection criterion of minimum total mission ΔV . The two types of missions selected are illustrated in figures 1 and 2. The conjunction class mission consists of two near-Hohmann transfers separated by an appropriate orbital stay of from 300 to 500 days. The opposition class missions are the so called "short-long" missions for which the outbound leg subtends a heliocentric transfer angle less than 180° , and the return leg swings inside the orbit of Venus and subtends an angle of about 300° .

The second step was simply to find the parking orbits which fit these missions. This step was accomplished by using the conic interplanetary mission planning program documented in reference 5. This program was modified by the authors to compute matched-conic solutions to the possible configurations of an elliptical regressing parking orbit at Mars. The fundamental ground rule for this part of the analysis was to find parking orbits which require no discrete propulsive maneuvers for orbital alinement. A complete discussion of the method of calculation of these orbits and the matching process is presented in references 3, 7, and 8.

The effect of the Earth orbital launch window, or mission window, and the resultant variations of the geometry of planetary approach and departure were also of interest. The primary interest was to see if the solutions would be uniform and predictable despite changes in the approach and departure asymptotes.

Matched-conic solutions for the minimum energy missions were calculated at 10-day increments through 50-day launch windows at Earth. The outbound and return flight times and the orbital stay time at Mars were held constant; thus, a 50-day transearth-injection (Earth-return) window at Mars was produced. There are various arguments for and against providing a return window at Mars; therefore, both a 50-day and a zero-day transearth or return launch window from Mars orbit are shown. The 50-day return window is shown by the solid lines of figure 3 and the zero-day return window is indicated by the dashed lines. Note that

the Earth entry velocity for the zero-day return window is constant. In the case of the zero-day return window, the orbital stay time is adjusted so that the launch from the Mars parking orbit always occurs at the same time, and the return leg of the mission is, of course, always the same. Providing a 50-day Earth-return window at Mars requires 1500 fps of additional ΔV .

Matched-conic solutions for the short-stay-time missions were calculated at 10-day increments through 40-day launch windows at Earth. The outbound and return flight times and the orbital stay time (30 days) at Mars were held constant. By holding the flight times constant, a 40-day Earth-return window at Mars was effectively produced. For these short missions there is no best time to leave Mars for a return to Earth. The best time to leave Mars is as soon as possible after arrival there. In other words, the velocity requirements for Mars departure and the Earth entry velocity are rapidly increasing with stay time, and the longer one remains in parking orbit, the more it costs to return home. The best stay is therefore zero days. For this study then, 30 days was somewhat arbitrarily chosen because this is the minimum orbital stay time which permits studying oblateness effects and the feasibility of using regressing parking orbits during short orbital missions to Mars.

Scanning Mars Orbital Missions Between 1975 and 1988

The results of the mission scan are presented in figures 4 and 5. These figures show the variation in mission velocity requirements from window to window and thereby facilitate direct comparison between both individual mission windows and both classes of missions. Although not shown in figure 5, there are nearly 100 days during the 1981, 1983, and 1984 short missions for which the velocity requirements are nearly minimum. The ΔV requirements for these wide mission windows are shown in more detail in figure 6(a) and (b). The least total mission ΔV requirements for the long missions occur for the launch opportunities in 1977 and 1979. For the short-stay-time mission the least total mission ΔV requirements occur during the 1983-84 and 1986 launch opportunities. The launch dates and trip times for these missions are summarized in tables I and II and figures 7 and 8.

The ΔV requirements shown in figures 3, 4, 5, and 6 are based on a simplified mission profile. Earth-orbital launch begins from a circular parking orbit at an altitude of 262 n. mi. The parking orbit is coplanar with the Earth departure hyperbola. The Mars-orbital insertion (MOI) and transearth injection (TEI) impulsive velocities are, of course, dependent on the type of parking orbit which is used at Mars. The MOI

and TEI impulsive velocities are shown for the highest energy regressing parking orbit, which shifts into alignment for departure and which is continuously available throughout the Earth orbital launch window. (The orbital elements of these orbits are illustrated later in figures 10 and 12.) The Earth entry velocity is shown for an entry altitude of 400 000 ft and a vacuum periapsis of 20 n. mi.

The minimum ΔV missions.— Certain important constraints were ignored during the search for the minimum ΔV missions. As stated earlier, minimum total mission ΔV was the only constraint used for mission selection. The most important constraint and the one most relevant to this report is the perihelion distance. In the case of the opposition class missions, this constraint is important because the spacecraft passes through the perihelion of the return trajectory as shown in figure 2. In these cases, perihelion is uncomfortably close to the sun.

To change the perihelion distance (at least for the case when the return trajectory is single impulse) would increase an already high ΔV requirement. As shown in figure 9, the perihelion radius is increasing with each launch opportunity, and in the middle and late 1980's not only have the velocity requirements reached their minimum value, but also the perihelion distance of the return trajectory has reached a more reasonable value, and in 1986 the spacecraft would pass just inside the orbital path of Venus during the return trip.

How Oblateness Affects the Parking Orbit Selection

Only secular rotation of the orbital plane and major axis due to planetary oblateness is considered. Orbital realignment is produced by rotation of the orbital line of nodes and the line of apsides, and these rotations are primarily the result of planetary oblateness. The rate of secular variation of the node and the periapsis vector is given by

$$\dot{\Omega}_s = \frac{-3nJ_2 R^2}{2a^2(1 - e^2)^2} \cos i \quad (1)$$

and

$$\dot{\omega}_s = \frac{-3nJ_2 R^2}{2a^2(1 - e^2)^2} \left(\frac{5}{2} \sin^2 i - 2 \right) \quad (2)$$

where

a	semimajor axis
e	orbital eccentricity
i	inclination with respect to the planetary equatorial plane
n	mean motion of the parking orbit
J_2	oblateness coefficient (assumed value for Mars = 0.002011) ^a
R	planetary equatorial radius
$\dot{\Omega}_s$	nodal regression rate
$\dot{\omega}_s$	periapsis precession rate

The term involving eccentricity divides out when the ratio of the rates ($\dot{\Omega}_s/\dot{\omega}_s$) is formed. This term merely scales or sizes the rates, and the ratio of the rates is determined by the orbital inclination. The important observation is that the eccentricity can be adjusted independently to change the rates while conserving a particular value of the ratio. The ability to change the eccentricity of the parking orbit is of great value when it is necessary to force the parking orbit to shift into alinement during arbitrarily short or long orbital stay times.

There is a definite connection between the characteristics of the parking orbit and the geometry of planetary approach and departure. The orbital inclination is determined by both this geometry and the ratio of the required angles of rotation of the orbital node and periapsis vectors, $\Delta\alpha_\Omega$ and $\Delta\omega_\rho$. The orbital inclination is determined so that the ratio of the orbital rotation rates, $\dot{\Omega}_s/\dot{\omega}_s$, is equal to the ratio of the required angles of rotation, $\Delta\alpha_\Omega/\Delta\omega_\rho$. The important effect is that orbital inclination will be frequently restricted to several relatively narrow bands across the region from 0° to 180°. Where these bands occur is, of course, dependent on the geometry of the planetary approach and departure asymptotes.

^aThe most recently adopted value of J_2 for Mars is given as 0.00197 in reference 9.

The stay time does not affect the inclination of the parking orbit, but it does affect the orbital eccentricity. For a given V_∞

geometry, as the stay time is shortened, accelerated rotation rates are required to insure final alinement with the departure asymptote, and progressively smaller orbital eccentricities are required to obtain the faster rates.

RESULTS

All data relating to the parking orbit at Mars is measured with respect to an inertial planetocentric coordinate system. The positive Z-axis of this coordinate system points north along the planetary axis of rotation. The XY-plane is defined by the planetary equatorial plane. The positive X-axis is defined by the intersection of the planetary orbit and equatorial planes and corresponds to the descending node of the planetary orbit on the equatorial plane. The positive Y-axis is 90° east of X and completes a right-handed system. The coordinate transformations between this system and appropriate geocentric and heliocentric systems are a part of the conic interplanetary mission planning program, and they are documented in reference 6.

Parking Orbits Available During Conjunction Class Missions

Eight to ten parking orbits were found during each long mission from 1975 to 1988. The orbits are summarized in table III. All the orbits for the long missions have periapsis altitudes of 200 n. mi. For these long missions, the orbits generally exhibit a range of eccentricities of from 0.3 to 0.9. The range of apoapsis altitudes is from 2000 to 28 000 n. mi. It should be noted that these orbits represent a set of the highest energy parking orbits which shift into alignment for departure. Each orbit, therefore, passes through the required angles of rotation of the orbital node and the periapsis vector only once. During the long stay-time missions, the parking orbits can be forced to complete a full revolution or multiple revolutions of either the orbital node or the periapsis vector prior to final alignment with the departure asymptote.

The parking orbits exhibit smooth variations and are available over a wide range of both the stay-time and the geometry of planetary approach and departure. The variations in the Keplerian orbital elements (a , e , i , Ω , and ω) are shown in figure 10 for a representative orbit which occurred during each long mission^a. The orbits shown in figure 10 are for the nominal mission; and the outbound flight-time, stay-time, and return flight-time for this mission are held constant and the launch date from earth orbit is varied. (The nominal mission is the mission at the center of the earth orbital launch window.) By holding the flight-time constant and varying the earth orbital launch date, changes were produced in the V_∞ vectors at both the time of

^aThe orbital elements are shown for an epoch corresponding to the time of the Mars orbital insertion maneuver which occurs at the time of periapsis passage on the approach hyperbola.

arrival and departure at Mars. The characteristics of the parking orbits must change to accommodate the variations in the geometry of planetary approach and departure.

Figure 10, therefore, shows the extent of the changes which can occur for the parking orbits listed in table III.

An important observation is that the parking orbits seem to take on characteristic values of inclination, and these inclinations are widely distributed as shown in table III. Also, the inclination varies smoothly and uniformly within narrow regions about the mean or characteristic value.

Another observation is that the orbital eccentricity is loosely correlated with the orbital inclination. The extent of this correlation is shown in figure 11. This figure displays the inclinations and apoapsis altitudes of representative orbits which were found during the long missions. There is a definite bucket-shaped region where orbits are not found. Note that low inclination orbits (both posigrade and retrograde with respect to the planetary axis of rotation) are possible but the frequency of finding them is less than for higher inclination orbits. (Perhaps by allowing a small discrete propulsive maneuver, these low inclination orbits could be found more frequently. This problem needs to be studied further.)

Parking Orbits Available During Opposition Class Missions

The technique appears to be feasible for short-stay orbital missions to Mars. For orbital stay times as low as 30 days, from five to eight parking orbits can be found; these orbits are summarized in table IV. All the orbits for the short missions have periapsis altitudes of 100 n. mi. The essential characteristic of the parking orbits for short-stay missions is that their range of eccentricities is not quite as large; many of the parking orbits are nearly circular. Although parking orbits can generally be found with orbital eccentricities between 0.4 and 0.7, these solutions begin disappearing as the stay time is shortened below 30 days. Solutions can generally be found for orbital stay times as low as 10 days. The technique does not work for stay times below 10 days except in those cases where periapsis vectors of the approach and departure asymptotes are already matched by some other technique, as in the case of a powered-turn flyby trajectory at Mars. In these instances, orbital eccentricities as high as 0.9 can be found.

The variations in the orbital elements (a , e , i , Ω , and ω) are shown in figure 12 for representative orbits which occurred during the short missions. Like the long mission, the orbits shown are for the nominal mission; and the flight time, stay time, and return flight time for this mission are held constant. The launch date from earth orbit is varied to produce changes in the V_{∞} vectors at both the time of arrival and departure at Mars. The characteristics of the parking orbits must, therefore, change to accommodate the resulting variations in the V_{∞} geometry.

The orbits appear to be more sensitive to changes in the V_{∞} geometry when the stay time is shortened. The inclinations generally correspond with those of the long missions, but there is greater fluctuation of the orbital elements, and the variations are not quite as smooth. The parking orbits may not be more sensitive to changes in the V_{∞} . In many of the short missions, the V_{∞} vectors are changing rapidly both in magnitude and direction, and the parking orbits must change more rapidly to accommodate these changes.

As was the case in the long missions, the orbital eccentricity is correlated with the orbital inclination. The extent of this relation is shown in figure 13, which displays the inclinations and apoapsis altitudes of representative orbits which were found for the short missions. The correlation appears to be even more definite than that seen for the long missions. Again, there is a definite bucket-shaped region where orbits are not found, but the solutions are much more closely grouped and widely distributed.

The Effect of Stay Time on the Parking Orbit

As mentioned in a preceding section, the stay time does not directly influence the inclination of the parking orbit, but it does affect the eccentricity. The effect of stay time is shown in figure 14. This figure shows the variation of orbital eccentricity with stay time for a hypothetical, nonvarying V_{∞} geometry. Three orbits were found to accommodate this geometry. Note that the eccentricity diminishes uniformly as the stay time is shortened until the solutions for the parking orbit disappear for stay times in the region of 20 to 40 days.

The region of stay times from 20 to 40 days is of great interest in the case of opposition class missions. For the study presented in this report, 30 days was selected for the stay time for all opposition class missions, and the questions arise: Can longer or shorter stay times be better; and, more important, can parking orbits be found if

the stay time is shortened below 30 days? To answer these questions, the opposition class mission in 1986 was chosen, and matched-conic simulations of this mission were performed for stay times of 10, 20, 30, and 40 days. The resulting parking orbits are tabulated in table V.

The most important observation is the number and selection of the parking orbits and their restriction to certain regions of inclination. The inclinations commonly occur near 25° , 51° , 75° , 130° and 150° . (The inclinations vary because of the changing geometry of departure.) Noteworthy is the fact that the missions with the shortest stay times have the lowest total mission ΔV requirements. Also, the parking orbit with the highest eccentricity and lowest velocity requirement is retrograde. This last observation is common to all the missions investigated in this report.

A second inspection of table V reveals the inclinations do not change greatly as the stay time is varied, despite the fact that the departure asymptote is changing. The worst thing that happens is that some solutions are lost or new solutions are found. This fact points out one of the limitations of the technique when it is used with the constraint that no plane changes are allowed: orbital inclinations smaller than the declination of either the approach or departure asymptotes are not possible without propulsive plane-change maneuvers.

The Correlation of Eccentricity and Inclination

It has been noted that the orbital inclination is determined so that the ratio of orbital rotation rates, $\dot{\Omega}_s/\dot{\omega}_s$, is equal to the ratio of the required angles of rotation, $\Delta\alpha_\Omega/\Delta\omega_\rho$. Therefore, the inclinations are determined by the geometry of planetary approach and departure (the quantity $\Delta\alpha_\Omega/\Delta\omega_\rho$) and by the characteristics of the orbital rotation rates. The result is that when the required angles of rotation are equal and in opposite directions, the rotation rates must likewise be equal and in opposite directions. This situation can occur at inclinations of 46.4° and 106.8° . Similarly, when the required angles of rotation are equal and in the same direction, the rotation rates must be equal and in the same direction. This situation occurs at inclinations of 73.2° and 133.6° .

As shown in tables III and IV, parking orbits aligned by oblateness often have inclinations near these equal-rate values. This is the case illustrated in figure 15, which shows the equal-rate inclinations super-imposed on a plot of the nodal and periapsis rotation rates. In addition, shaded bands are shown indicating the inclinations where parking orbits are commonly found. That there is a definite relationship between the inclination and eccentricity is indicated by this figure.

Consider two parking orbits with identical nodal and periapsis rotation rates - one a near-polar orbit and the other a near-equatorial orbit. The near-equatorial orbit has the larger eccentricity. For example, if two orbits have inclinations of 46.4° and 106.8° (the inclinations for which the rates are equal and opposite), the orbit with the 46.4° inclination has higher rotation rates than the one with a 106.8° inclination. Thus, the eccentricity of the orbit inclined must be increased to slow its rates enough to match those of the orbit inclined 106.8° .

These considerations combine to limit the regions of occurrence of regressing parking orbits; and the correlation of eccentricity is strikingly evident if we examine any mission in detail.

In figure 16, the characteristics of parking orbits which occur during the 1977 conjunction class mission are shown; and the apoapsis altitude is plotted against orbital inclination. The regions where parking orbits commonly occur are indicated by the shaded bars. The width of the bar indicates the region of inclinations where solutions are commonly found. The height of the bar shows the range of apoapsis altitudes which are commonly found for the highest energy parking orbits (i.e., orbits that shift through the required angles only once). The bars therefore indicate the upper bound of the orbital apoapsis altitude. Orbits with lower apoapsis altitudes can be found by requiring the node or periapsis of the parking orbit to shift through integral multiples of 2π prior to final alignment with the departure asymptote. The orbits found during this mission are summarized in detail in table VI.

The apoapsis altitudes and inclinations of orbits which occur during the 1986 opposition class mission are plotted in figure 17. Again, the shaded bars indicate the regions where the data points tend to occur. The orbits found during this mission are summarized in detail in table VII.

CONCLUDING REMARKS

The use of gravitational perturbations for parking orbit alinement appears to be useful in the areas of mission analysis and trajectory definition for both the long and short missions to Mars. For both types of missions, the orbital inclinations fall into narrow bands which are widely distributed over the interval of possible inclinations. Also, the orbital eccentricity is correlated with the orbital inclination, and, in general, parking orbits with low inclinations have high eccentricities. Also, the parking orbits often have remarkably high orbital eccentricities, indicating that even with very small rates of rotation, the orbital node and line of apsides need not shift through large angles to effect orbital alinement. One cannot therefore discount the effects of oblateness on the parking orbit even when those effects are small.

For both types of missions the highest energy orbits have low inclinations and can be either posigrade or retrograde with respect to the planetary axis of rotation. The highest energy orbits always have very low inclinations and are retrograde.

For the long stay-time orbital missions to Mars, a wide selection (from 6 to 11) of possible parking orbits is available. These parking orbits exhibit smooth variations in characteristics and are available over a wide range of both stay time and the geometry of planetary approach and departure. The range of eccentricities is generally from 0.4 to 0.8.

For the short stay-time missions, the use of gravitational perturbations for alinement is more limited, but is nevertheless useful since a number of orbits are generally available. Although there are fewer orbits available (from 3 to 7), the parking orbits for the short missions exhibit a wider variation of both the inclination and eccentricity. The orbits appear to be more sensitive to changes in the V_{∞} geometry for the short stay-time missions. The inclinations correspond to those of the long missions. The range of eccentricities is generally from 0.0 to 0.7.

The greatest number of orbits have high inclinations near 70° . These orbits are found for any V_{∞} geometry and are available during each mission that was investigated. These orbits are nearly circular for most of the short missions. They exhibit moderate eccentricities (from 0.3 to 0.5) for the long missions.

TABLE I.- EARTH-ORBITAL LAUNCH DATES AND TRIP TIMES
FOR MINIMUM ΔV MISSIONS TO MARS

Calendar date of launch from Earth parking orbit	Julian date of launch, (add 2 440 000)	Outbound flight time, days	Mars arrival date, (add 2 440 000)	Stay time, days	Return flight time, days	Total trip time, days
Aug 29, 1975	2 629	349	2 978	376	283	1 008
	2 654	349	3 003	351	283	983
	2 679	349	3 028	326	283	958
Oct 15, 1977	3 407	332	3 739	358	326	1 016
	3 432	332	3 764	333	326	991
	3 457	332	3 789	308	326	966
Nov 26, 1979	4 148	314	4 462	409	333	1 056
	4 173	314	4 487	384	333	1 031
	4 198	314	4 512	359	333	1 006
Nov 21, 1981	4 905	302	5 207	441	314	1 057
	4 930	302	5 232	416	314	1 032
	4 955	302	5 257	391	314	1 007
Dec 21, 1983	5 665	280	5 945	528	220	1 028
	5 690	280	5 970	503	220	1 003
	5 715	280	5 995	478	220	978
May 4, 1986	6 530	200	6 730	565	200	965
	6 555	200	6 755	540	200	940
	6 580	200	6 780	515	200	915
July 10, 1988	7 328	200	7 528	565	270	1 035
	7 353	200	7 553	540	270	1 010
	7 378	200	7 578	515	270	985

TABLE II.- EARTH-ORBITAL LAUNCH DATES AND TRIP TIMES
FOR SHORT STAY TIME MISSIONS TO MARS

Calendar date of launch from Earth parking orbit	Julian date of launch, (add 2 440 000)	Outbound flight time, days	Mars arrival date, (add 2 440 000)	Stay time, days	Return flight time, days	Total trip time, days
Sept 4, 1975	2 640	210	2 850	30	240	480
	2 660	210	2 870	30	240	480
	2 680	210	2 890	30	240	480
Oct 13, 1977	3 410	210	3 620	30	230	470
	3 430	210	3 640	30	230	470
	3 450	210	3 660	30	230	470
Nov 22, 1979	4 180	240	4 420	30	210	480
	4 200	240	4 440	30	210	480
	4 220	240	4 460	30	210	480
Nov 11, 1981	4 900	260	5 160	30	220	510
	4 920	260	5 180	30	220	510
	4 940	260	5 200	30	220	510
Dec 31, 1981	4 950	220	5 170	30	220	470
	4 970	220	5 190	30	220	470
	4 990	220	5 210	30	220	470
Dec 21, 1983	5 670	260	5 930	30	230	520
	5 690	260	5 950	30	230	520
	5 710	260	5 970	30	230	520
Feb 29, 1984	5 740	200	5 940	30	230	460
	5 760	200	5 960	30	230	460
	5 780	200	5 980	30	230	460
Apr 29, 1986	6 530	180	6 710	30	250	460
	6 550	180	6 730	30	250	460
	6 570	180	6 750	30	250	460
July 7, 1988	7 330	160	7 490	30	260	450
	7 350	160	7 510	30	260	450
	7 370	160	7 530	30	260	450

TABLE III.- SUMMARY OF MARS PARKING ORBITS WHICH OCCURRED
DURING THE CONJUNCTION CLASS MISSIONS

Orbit no.	Inclination, deg	Apoapsis altitude, n. mi.	Period, hr	Eccentricity	Mars orbit insertion ΔV , fps	Transearth injection ΔV , fps	Total mission ΔV , fps
(a) Earth departure date, August 25, 1975							
1	69.88	5 664.12	7.00	.57	3745.98	4394.34	20 768.81
2	144.10	9 313.21	11.38	.69	3234.95	3883.76	19 748.07
3	72.78	2 441.15	3.78	.35	4742.58	5390.96	22 762.05
4	68.06	5 744.77	7.09	.58	3731.22	4378.49	20 738.77
5	142.27	7 828.35	9.51	.65	3403.25	4051.52	20 084.41
6	69.91	2 581.91	3.90	.37	4677.04	5324.37	22 630.49
(b) Earth departure date, October 13, 1977							
1	16.75	12 046.59	15.09	.74	3007.19	3247.25	18 106.61
2	69.29	5 480.15	6.80	.56	3780.57	4020.60	19 653.35
3	112.14	4 402.88	5.66	.51	4034.15	4274.22	20 160.61
4	142.33	8 104.31	9.85	.66	3365.93	3606.04	18 824.26
5	71.67	2 386.66	3.73	.35	4766.75	5008.10	21 627.03
6	18.67	11 616.71	14.48	.74	3037.36	3277.49	18 167.04
7	69.15	5 490.10	6.81	.56	3779.64	4019.85	19 651.74
8	112.25	4 407.92	5.67	.51	4033.91	4274.15	20 160.38
9	142.31	8 031.32	9.76	.66	3375.61	3615.85	18 843.80
10	71.32	2 405.14	3.75	.35	4758.77	4997.67	21 608.71
11	172.93	20 335.60	28.28	.83	2646.14	2886.18	17 384.64
(c) Earth departure date, October 26, 1979							
1	24.59	10 835.68	13.40	.72	3335.41	3034.58	18 023.93
2	68.06	6 283.96	7.70	.60	3869.03	3567.97	19 091.27
3	113.19	4 930.34	6.21	.54	4142.31	3841.11	19 637.89
4	141.48	8 170.44	9.93	.66	3598.16	3296.95	18 549.59
5	71.07	2 802.53	4.11	.39	4815.50	4515.12	20 984.91
6	70.62	6 104.13	7.49	.59	3900.94	3600.36	19 154.99
7	111.28	4 851.08	6.13	.53	4161.23	3860.52	19 675.64
8	141.94	9 559.44	11.70	.70	3448.89	3148.01	18 251.02
9	72.06	2 746.55	4.05	.38	4839.92	4538.64	21 032.26
(d) Earth departure date, November 21, 1981							
1	68.52	7 117.15	8.66	.63	4412.74	3307.77	19 420.14
2	139.76	8 241.85	10.02	.66	4265.86	3160.65	19 126.48
3	56.87	4 727.33	5.00	.53	4866.09	3761.76	20 327.34
4	70.24	3 174.68	4.45	.42	5341.46	4237.15	21 278.27
5	70.63	6 985.30	8.51	.62	4432.33	3327.99	19 459.03
6	140.39	9 422.43	11.52	.69	4138.33	3033.45	18 871.23
7	29.09	9 948.74	12.21	.70	4086.58	2982.04	18 767.44
8	73.14	3 002.81	4.29	.41	5408.67	4303.63	21 411.00

TABLE III.- SUMMARY OF MARS PARKING ORBITS WHICH OCCURRED
DURING THE CONJUNCTION CLASS MISSIONS - Concluded

Orbit no.	Inclination, deg	Apoapsis altitude, n. mi.	Period, hr	Eccentricity	Mars orbit insertion ΔV , fps	Transearth injection ΔV , fps	Total mission ΔV , fps
(e) Earth departure date, December 21, 1983							
1	37.30	13 205.13	16.76	.76	4744.30	2837.97	19 709.10
2	137.13	7 762.90	9.43	.65	5219.44	3312.26	20 659.82
3	56.99	6 267.01	7.68	.60	5441.82	3535.99	21 105.01
4	71.62	4 020.42	5.28	.48	5951.55	4045.65	22 124.65
5	142.03	17 780.30	23.93	.81	4537.72	2631.04	19 296.87
6	74.59	8 987.64	10.96	.68	5075.16	3169.13	20 370.93
7	135.71	10 079.20	12.38	.71	4971.20	3064.54	20 163.34
8	58.85	6 478.30	7.92	.61	5406.12	3499.46	21 032.08
9	72.95	3 927.06	5.18	.48	5979.75	4072.91	22 179.29
(f) Earth departure date, May 4, 1986							
1	77.15	11 453.44	14.25	.73	4178.40	4180.48	19 887.11
2	132.82	8 885.22	10.83	.68	4405.80	4407.78	20 341.94
3	55.27	7 449.45	9.06	.64	4578.76	4580.52	20 687.32
4	72.03	4 662.80	5.93	.52	5095.63	5097.39	21 721.21
5	102.10	6 471.64	7.91	.61	4726.98	4728.75	20 984.10
6	135.40	14 187.03	18.23	.77	4010.93	4012.93	19 552.00
7	36.94	16 928.05	22.53	.80	3887.02	3888.54	19 302.73
8	134.69	7 439.10	9.04	.64	4581.43	4582.92	20 691.92
9	58.16	7 895.18	9.60	.65	4520.38	4522.05	20 569.55
10	74.01	4 485.83	5.75	.51	5141.40	5143.07	21 811.60
11	132.36	19 746.91	27.26	.83	3792.04	3793.71	19 113.29
(g) Earth departure date, July 10, 1988							
1	137.56	9 562.15	11.70	.70	3376.60	4925.71	20 279.93
2	58.01	6 627.48	8.09	.61	3739.95	5289.17	21 006.32
3	72.14	4 185.40	5.44	.49	4261.82	5811.24	22 050.29
4	97.38	6 638.04	8.10	.61	3738.71	5288.34	21 004.38
5	150.87	27 807.85	42.33	.87	2652.55	4201.87	18 832.14
6	137.52	9 614.52	11.77	.70	3372.81	4921.09	20 272.04
7	57.86	6 616.26	8.08	.61	3743.27	5290.49	21 011.63
8	72.03	4 194.01	5.45	.49	4261.07	5808.26	22 047.30
9	97.49	6 686.85	8.16	.61	3732.67	5279.98	20 990.75
10	149.70	26 225.53	39.20	.86	2680.83	4228.99	18 887.92

TABLE IV.- SUMMARY OF MARS PARKING ORBITS WHICH OCCURRED
DURING THE OPPOSITION CLASS MISSIONS

Orbit no.	Inclination, deg	Apoapsis altitude, n. mi.	Period, hr	Eccentricity	Mars orbit insertion ΔV , fps	Transearth injection ΔV , fps	Total mission ΔV , fps
(a) Earth departure date, September 14, 1975							
1	62.70	2 418.52	3.67	.37	6725.35	20 450.99	40 147.16
2	139.86	10 141.12	12.33	.72	5141.09	18 866.91	36 979.56
3	51.92	198.05	1.89	.02	8536.32	22 261.32	43 768.05
4	133.23	716.07	2.27	.14	7925.23	21 650.62	42 547.32
5	81.49	1 450.51	2.84	.26	7298.89	21 022.72	41 293.74
6	53.41	274.85	1.94	.04	8434.68	22 159.12	43 565.60
7	131.82	930.78	2.43	.18	7719.13	21 444.10	42 135.54
(b) Earth departure date, November 2, 1977							
1	34.36	3 308.90	4.49	.45	7098.40	20 851.11	41 318.11
2	67.57	2 338.29	3.60	.37	7512.98	21 266.11	42 147.43
3	50.88	124.75	1.84	.01	9387.05	23 139.48	45 894.99
4	135.12	635.11	2.21	.12	8756.96	22 510.22	44 635.48
5	77.22	1 841.43	3.17	.31	7787.68	21 540.17	42 696.92
6	131.45	1 189.80	2.63	.22	8243.66	21 997.26	43 609.74
(c) Earth departure date, November 22, 1979							
1	72.13	1 796.07	3.13	.30	7052.34	18 726.60	37 775.97
2	135.74	672.04	2.23	.13	7955.15	19 629.92	39 582.07
3	72.98	1 756.35	3.10	.30	7076.11	18 750.89	37 824.62
4	55.77	222.54	1.91	.03	8486.96	20 161.92	40 646.49
5	131.32	1 357.78	2.77	.24	7349.68	19 025.52	38 372.63
(d) Earth departure date, November 11, 1981							
1	72.45	1 846.64	3.17	.31	8043.35	15 840.14	36 096.80
2	136.03	590.89	2.17	.11	9063.72	16 861.44	38 138.87
3	72.21	1 857.48	3.18	.31	8036.99	15 833.48	36 082.52
4	22.28	2 987.34	4.18	.43	7480.13	15 276.19	34 968.74
5	56.14	252.20	1.93	.04	9470.42	17 266.77	38 949.20
6	130.75	1 455.19	2.85	.26	8301.47	16 099.08	36 613.55
(e) Earth departure date, December 31, 1981							
1	78.72	1 833.02	3.16	.31	8306.52	16 582.10	36 803.54
2	50.99	155.63	1.86	.01	9856.81	18 132.11	39 903.46
3	134.38	632.57	2.20	.12	9273.76	17 550.20	38 738.75
4	37.09	3 393.90	4.57	.46	7579.73	15 856.64	35 350.43
5	54.28	304.59	1.96	.05	9654.68	17 931.92	39 500.54
6	131.11	1 071.18	2.54	.20	8854.38	17 132.29	37 900.64
(f) Earth departure date, December 21, 1983							
1	74.65	2 678.76	3.90	.40	6930.63	14 653.06	33 921.48
2	49.79	111.36	1.83	.00	8984.66	16 707.60	38 029.51
3	133.81	390.15	2.03	.07	8615.78	16 338.90	37 293.09
4	79.50	2 217.31	3.49	.35	7153.96	14 877.07	34 367.50
5	56.14	413.04	2.04	.07	8586.50	16 308.97	37 231.75
6	127.03	1 039.54	2.52	.19	7948.57	15 671.22	35 957.15

TABLE IV.- SUMMARY OF MARS PARKING ORBITS WHICH OCCURRED
DURING THE OPPOSITION CLASS MISSIONS - Concluded

Orbit no.	Inclination, deg	Apoapsis altitude, n. mi.	Period, hr	Eccentricity	Mars orbit insertion ΔV , fps	Transearth injection ΔV , fps	Total mission ΔV , fps
(g) Earth departure date, February 29, 1984							
1	87.50	1845.41	3.26	.29	7576.74	15 854.30	35 675.77
2	50.07	244.04	1.99	.01	9003.52	17 281.75	38 529.82
3	39.94	4757.92	6.03	.53	6454.89	14 733.64	33 432.03
4	72.53	4786.90	6.06	.53	6448.29	14 727.38	33 418.96
5	52.27	370.09	2.08	.04	8843.02	17 121.33	38 207.76
(h) Earth departure date, April 19, 1986							
1	83.70	1803.71	3.14	.30	6884.85	14 446.12	32 784.75
2	52.91	337.53	1.99	.06	8174.84	15 736.77	35 365.12
3	129.91	691.40	2.25	.13	7772.80	15 334.91	34 561.66
4	31.33	3959.02	5.12	.50	5957.45	13 519.13	30 929.41
5	71.62	3259.53	4.44	.45	6190.66	13 752.58	31 396.05
6	148.67	9186.96	11.09	.70	5052.50	12 614.44	29 120.40
7	51.89	289.46	1.95	.05	8236.33	15 797.48	35 486.59
8	130.98	603.72	2.18	.11	7865.59	15 426.94	34 745.80
(i) Earth departure date, June 27, 1988							
1	70.32	1265.21	2.69	.23	8080.41	14 650.97	35 010.69
2	14.49	2463.51	3.71	.38	7348.41	13 918.26	33 545.72
3	136.03	1851.36	3.18	.31	7678.64	14 250.46	34 208.81
4	162.53	9321.11	11.26	.70	5861.24	12 432.95	30 573.98
5	70.44	1261.67	2.69	.23	8084.00	14 654.20	35 017.48
6	138.30	955.76	2.45	.18	8340.51	14 911.45	35 531.65

TABLE V.- THE NUMBER AND SELECTION OF PARKING ORBITS AND THEIR DEPENDENCE
ON THE ORBITAL STAY DURING THE 1986 OPPOSITION CLASS MISSION

Orbital stay time, day	Orbit no.	Inclination, deg	Eccentricity	Apoapsis altitude, n. mi.	Longitude of ascending node, deg	Argument of perapsis, deg	Mars orbit insertion ΔV , fps	Transearth injection ΔV , fps	Total mission ΔV , fps
40	1	52.39	.1646	865	184.88	315.65	7345	15 894	34 706
	2	128.53	.1882	1001	204.27	315.83	7223	15 772	34 462
	3	21.08	.6128	6254	48.22	84.63	5182	13 730	30 378
	4	158.90	.6640	7783	340.65	84.62	4958	13 506	29 930
	5	50.93	.1484	777	24.44	104.61	7431	15 978	34 874
	6	129.97	.1696	894	4.08	104.39	7320	15 868	34 655
30	1	52.67	.0650	370	185.00	315.58	7880	15 933	35 280
	2	129.37	.1196	628	204.57	316.03	7585	15 639	34 690
	3	25.10	.5179	4278	41.65	90.67	5612	13 665	30 742
	4	75.83	.4708	3559	17.53	107.79	5831	13 884	31 181
	5	154.87	.6545	7463	347.21	90.66	5000	13 053	29 518
	6	51.72	.0546	324	24.17	104.79	7937	15 990	35 393
	7	130.37	.1052	557	3.92	104.29	7663	15 715	34 844
20	1	130.23	.0165	165	204.89	316.23	8151	15 732	35 349
	2	28.89	.3849	2532	37.27	94.58	6238	13 819	31 523
	3	151.08	.6371	6925	351.58	94.56	5077	12 657	29 200
	4	130.82	.0070	127	3.75	104.18	8205	15 785	35 456
10	1	32.29	.1595	837	34.25	97.18	7373	14 487	33 324
	2	147.68	.5927	5758	354.61	97.17	5274	12 389	29 129

TABLE VI.- SUMMARY OF REGRESSING PARKING ORBITS WHICH SHIFT INTO ALIGNMENT

DURING THE 1977 CONJUNCTION CLASS MISSION

Orbit no.	Inclination, deg	Eccentricity	Apoapsis altitude, n. mi.	Longitude of ascending node, deg	Argument of perapsis, deg	Mars orbit insertion ΔV , fps	Transearth injection ΔV , fps	Total mission ΔV , fps
(a) Launch date from earth parking orbit, September 23, 1977								
1	7.75	.7752	14 295	357.45	354.87	2782	3115	17 980
2	17.32	.7547	12 774	23.22	329.61	2867	3200	18 150
3	69.40	.5713	5 648	38.58	317.15	3654	3986	19 724
4	111.90	.5223	4 669	42.72	317.19	3872	4205	20 161
5	142.88	.6758	8 721	47.62	320.28	3202	3534	18 820
6	71.69	.3613	2 512	38.81	317.07	4613	4947	21 643
7	22.15	.7340	11 480	233.80	117.24	2954	3287	18 324
8	68.93	.5727	5 679	222.63	125.76	3648	3981	19 713
9	112.27	.5232	4 686	218.38	125.71	3869	4202	20 155
10	142.75	.6687	8 453	213.54	122.65	3233	3565	18 882
11	71.21	.3639	2 539	222.39	125.84	4601	4933	21 618
(b) Launch date from earth parking orbit, October 13, 1977								
1	16.75	.7436	12 046	26.58	321.77	3007	3247	18 106
2	69.29	.5636	5 480	36.07	314.01	3780	4020	19 653
3	112.14	.5069	4 403	38.58	314.04	4034	4274	20 160
4	142.33	.6591	8 104	41.43	315.83	3365	3606	18 824
5	71.67	.3485	2 386	36.22	313.96	4766	5008	21 627
6	18.66	.7363	11 617	226.83	120.54	3037	3277	18 167
7	69.15	.5641	5 490	218.51	127.15	3779	4019	19 652
8	112.25	.5072	4 408	215.96	127.11	4034	4279	20 160
9	142.30	.6570	8 031	213.12	125.33	3375	3615	18 843
10	71.31	.3504	2 405	218.37	127.20	4758	4997	21 608
11	172.93	.8312	20 335	190.45	103.58	2646	2886	17 384

TABLE VI.- SUMMARY OF REGRESSING PARKING ORBITS WHICH SHIFT INTO ALINEMENT

DURING THE 1977 CONJUNCTION CLASS MISSION - Concluded

Orbit no.	Inclination, deg	Eccentricity	Apoapsis altitude, n. mi.	Longitude of ascending node, deg	Argument of periapsis, deg	Mars orbit insertion ΔV , fps	Transearth injection ΔV , fps	Total mission ΔV , fps
(c) Launch date from earth parking orbit, November 12, 1977								
1	20.07	.6936	9455	62.76	265.51	4136	3457	20 902
2	141.25	.6132	6679	10.81	283.84	4481	3804	21 595
3	58.24	.4574	3645	34.14	289.14	5177	4499	22 987
4	94.62	.5081	4423	25.42	291.30	4946	4269	22 526
5	111.87	.4766	3922	211.42	136.70	5089	4413	22 809
6	141.48	.6459	7656	222.16	143.34	4340	3664	21 311
7	59.16	.4603	3686	199.05	137.79	5163	4485	22 957
8	94.13	.4914	4150	207.35	135.76	5021	4343	22 672

TABLE VII.- SUMMARY OF REGRESSING PARKING ORBITS WHICH SHIFT INTO ALIGNMENT

DURING THE 1986 OPPOSITION CLASS MISSION

Orbit no.	Inclination, deg	Eccentricity	Apoapsis altitude, n. mi.	Longitude of ascending node, deg	Argument of periapsis, deg	Mars orbit insertion ΔV , fps	Transearth injection ΔV , fps	Total mission ΔV , fps
(a) Launch date from earth parking orbit, April 19, 1986								
1	83.70	.3047	1804	193.78	313.30	6885	14 446	32 785
2	52.91	.0576	337	184.36	316.91	8175	15 737	35 365
3	129.91	.1320	691	207.59	317.66	7773	15 335	34 562
4	31.33	.4981	3959	39.88	90.94	5957	13 519	30 929
5	71.61	.4483	3259	20.20	104.07	6190	13 752	31 396
6	148.67	.7003	9187	350.87	90.91	5052	12 614	29 120
7	51.89	.0465	289	26.80	100.89	8236	15 797	35 486
8	130.98	.1147	603	2.71	100.08	7865	15 427	34 745
(b) Launch date from earth parking orbit, April 29, 1986								
1	86.53	.3420	2120	192.65	311.16	6262	14 744	32 524
2	52.36	.0734	408	185.54	313.77	7649	16 131	35 299
3	128.90	.1073	567	201.35	314.00	7466	15 948	34 934
4	19.19	.5384	4635	43.25	89.84	5334	13 815	30 666
5	81.33	.4829	3732	14.79	111.27	5590	14 072	31 179
6	51.49	.0638	364	21.22	108.61	7702	16 183	35 403
7	129.80	.0955	510	4.94	108.35	7530	16 011	35 059
(c) Launch date from earth parking orbit, May 9, 1986								
1	86.18	.3728	2410	197.87	306.63	6746	14 456	33 120
2	52.07	.0765	422	191.76	308.90	8266	15 977	36 160
3	129.17	.1094	577	205.43	309.09	8089	15 800	35 807
4	15.50	.5540	4930	50.96	84.63	5896	13 606	31 420
5	82.14	.4845	3753	19.62	109.55	6217	13 927	32 061
6	164.47	.6335	6820	345.94	84.63	5541	13 252	30 710
7	51.12	.0657	373	25.35	107.19	8326	16 035	36 278
8	130.16	.0963	514	11.21	106.98	8160	15 870	35 948

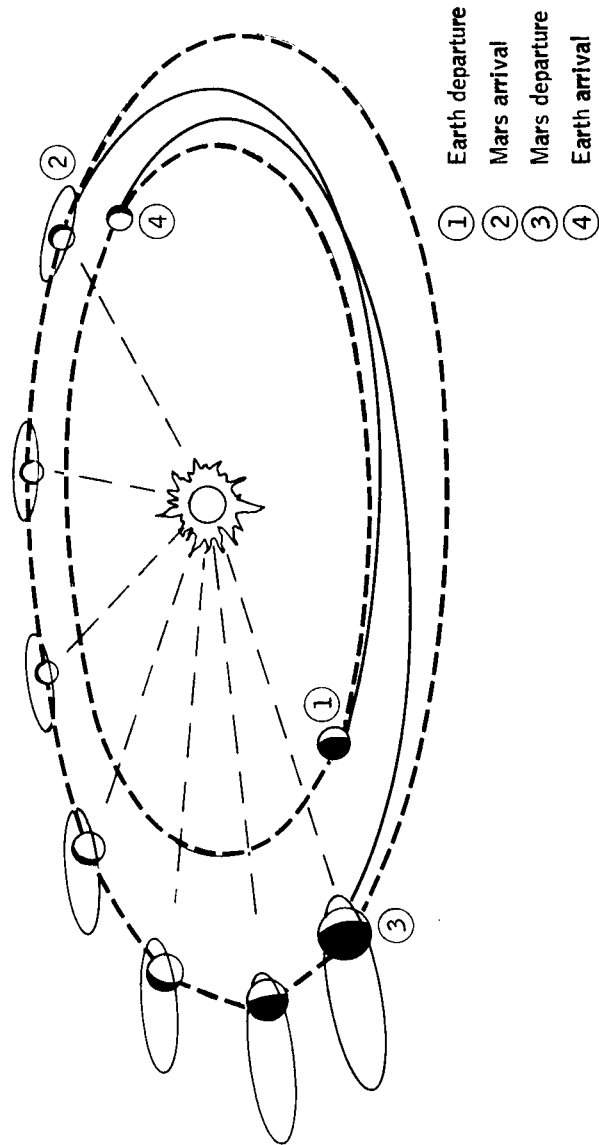


Figure 1.- Heliocentric schematic illustrating the conjunction class mission and the parking orbit about Mars.

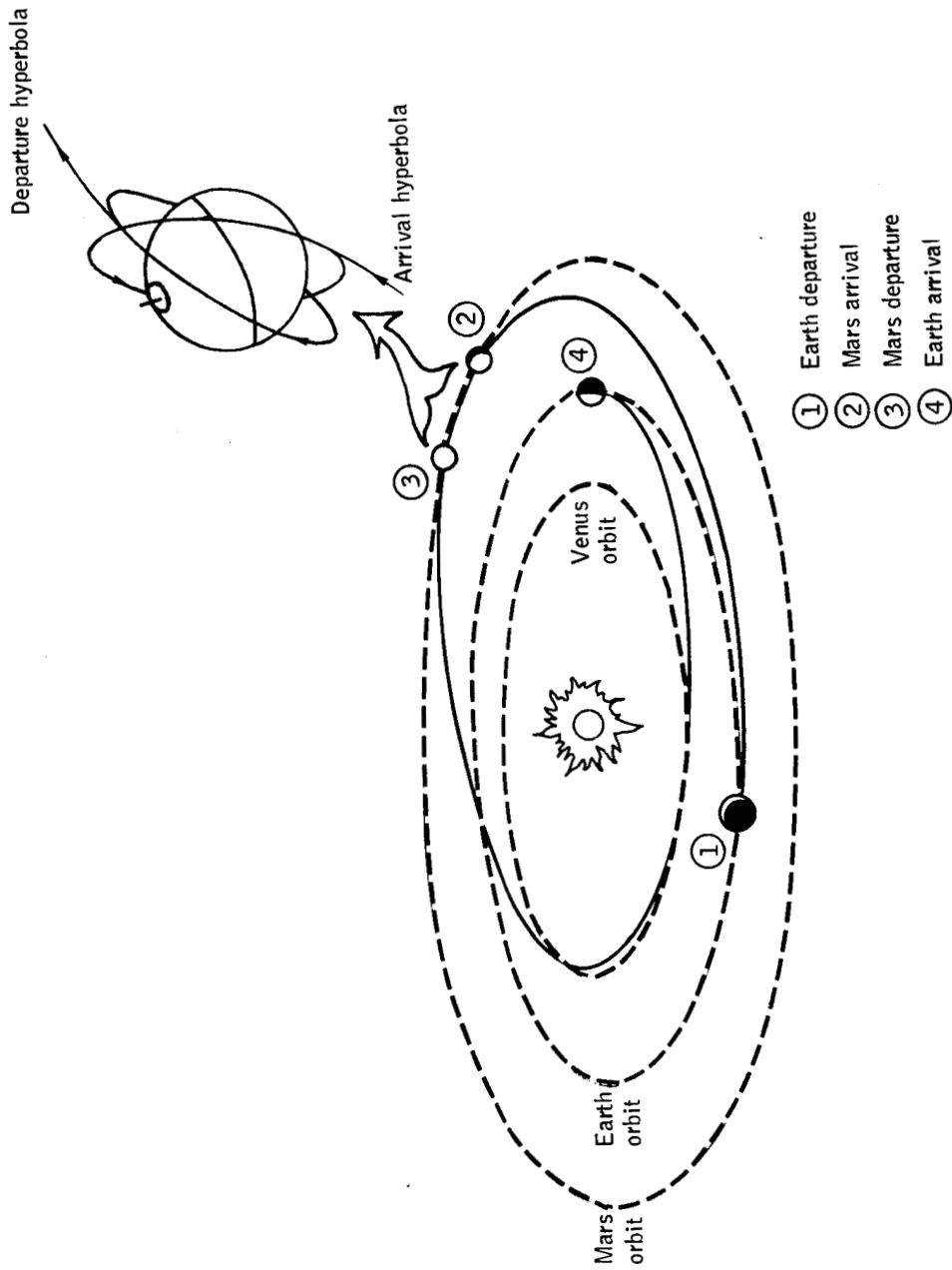
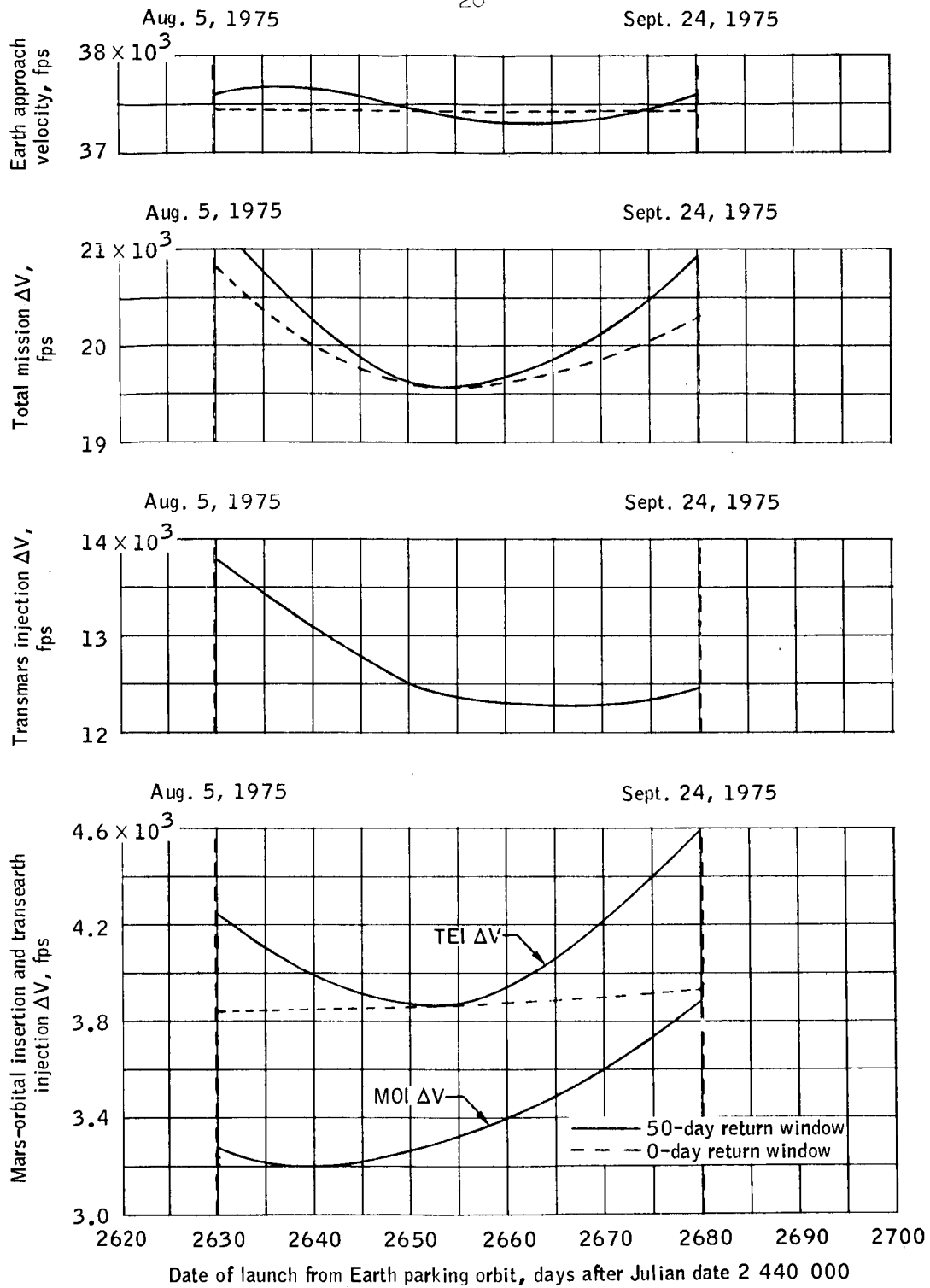
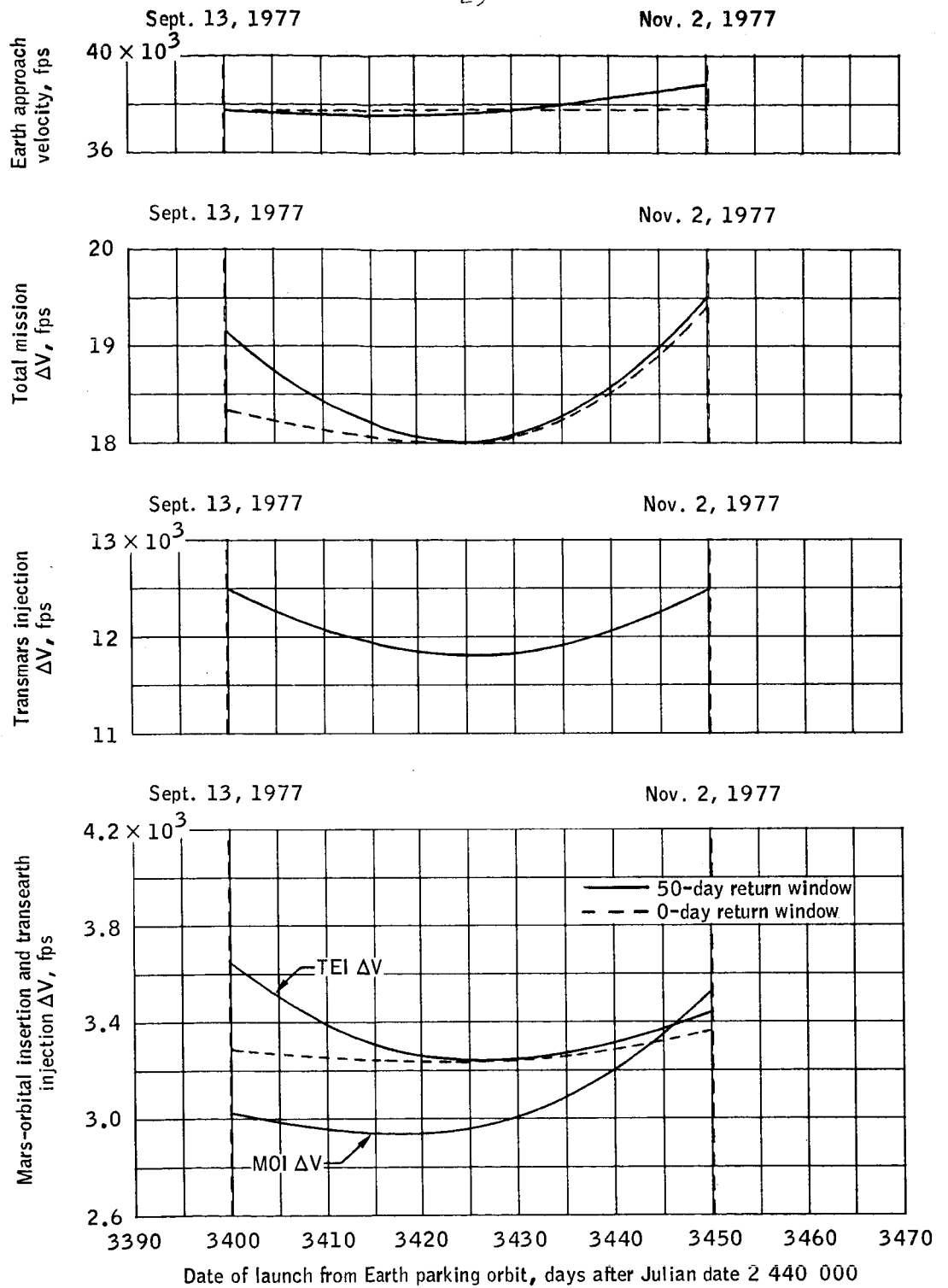


Figure 2.- Heliocentric schematic illustrating the opposition class mission and the parking orbit about Mars.



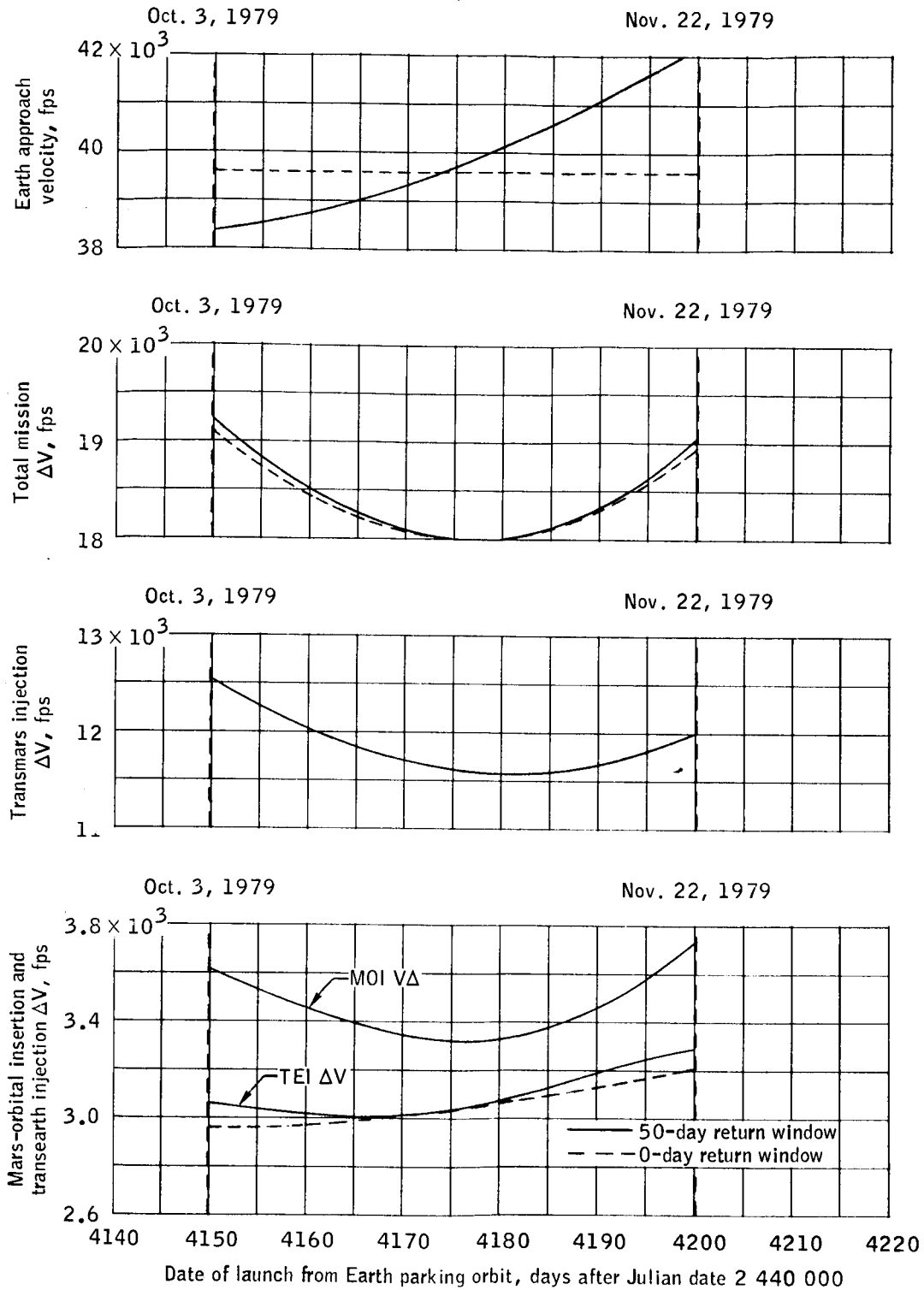
(a) The 1975 mission window.

Figure 3.- The variation of mission velocity requirements for minimum ΔV missions.



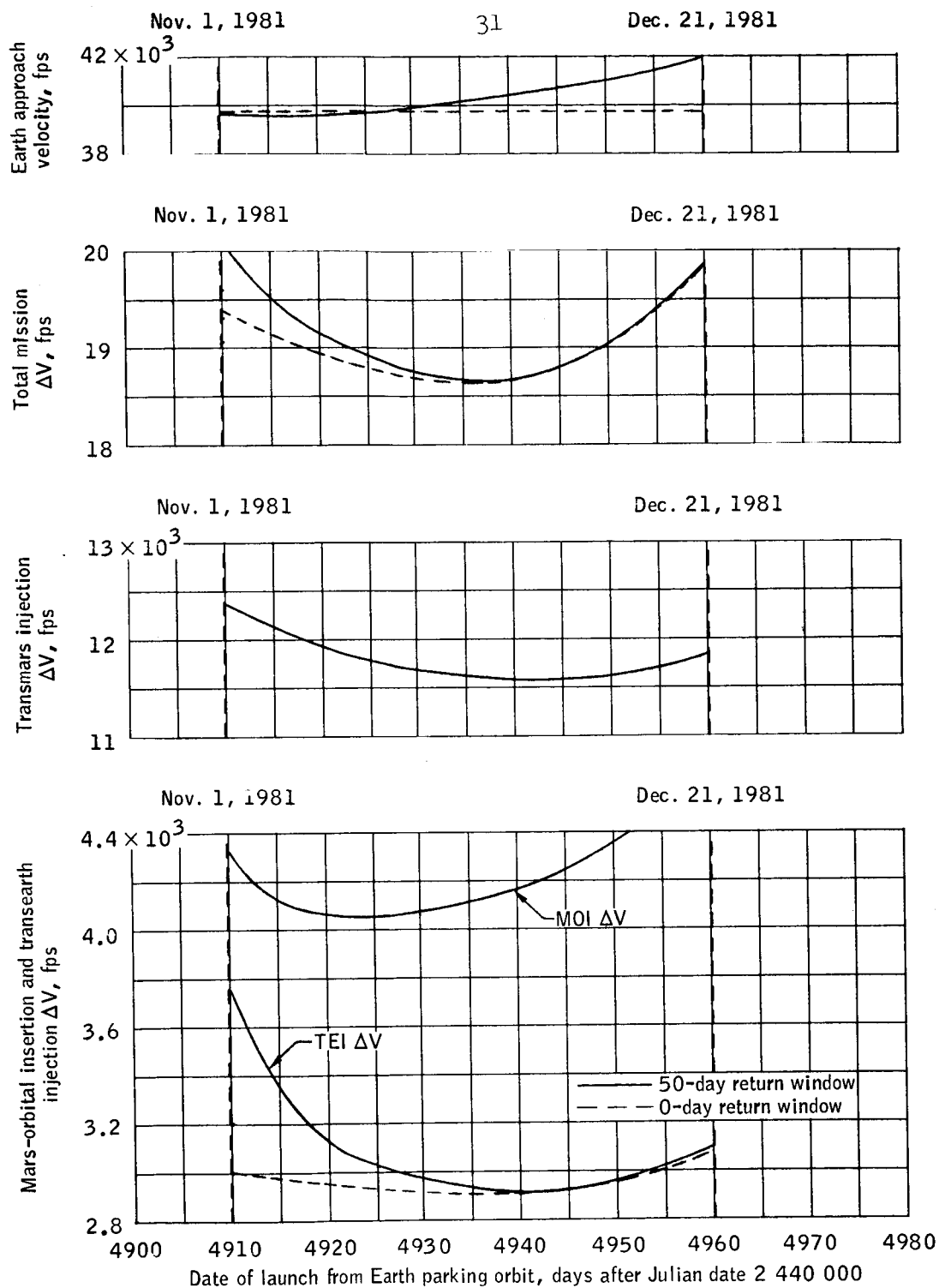
(b) The 1977 mission window.

Figure 3.- Continued.



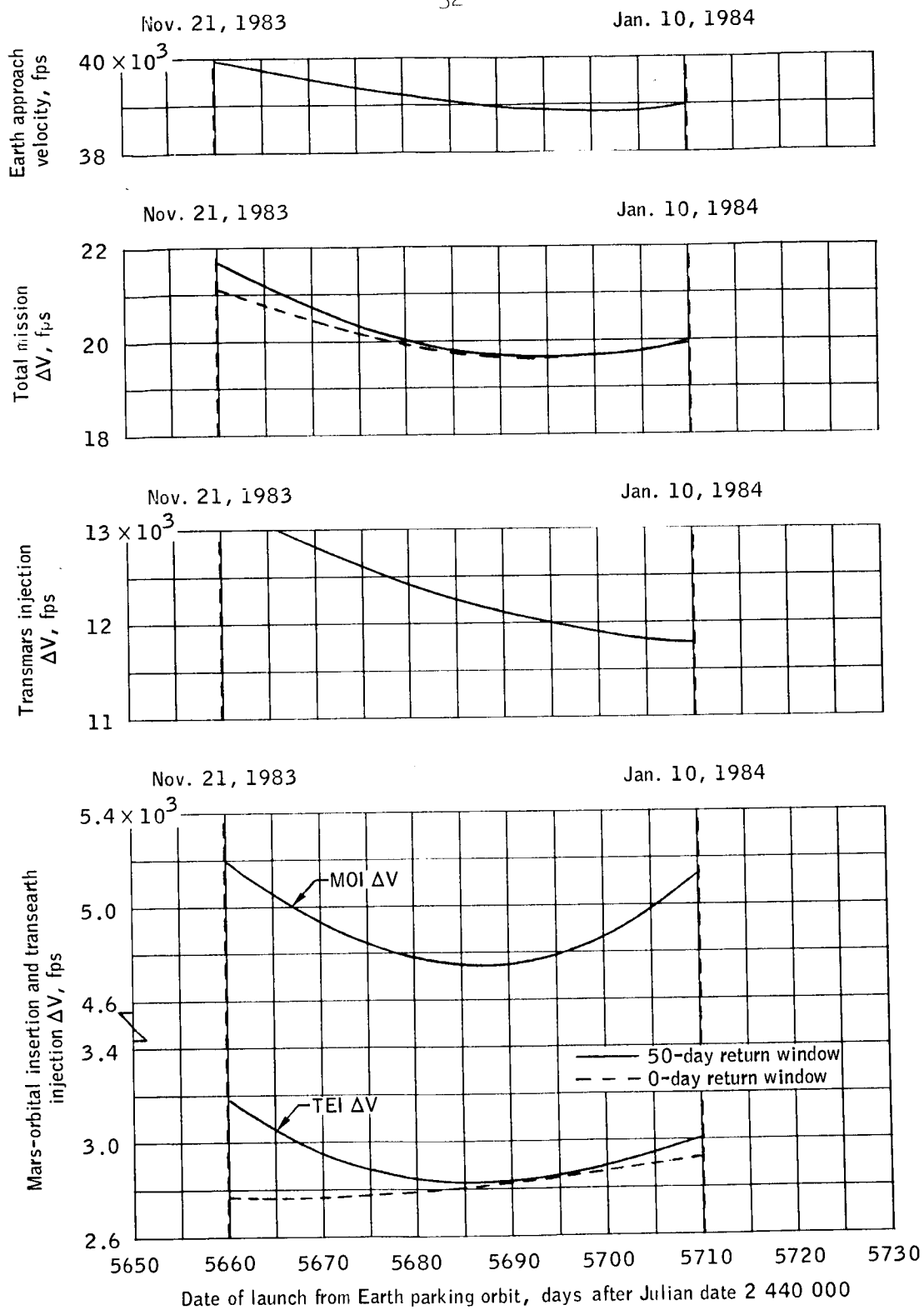
(c) The 1979 mission window.

Figure 3.- Continued.



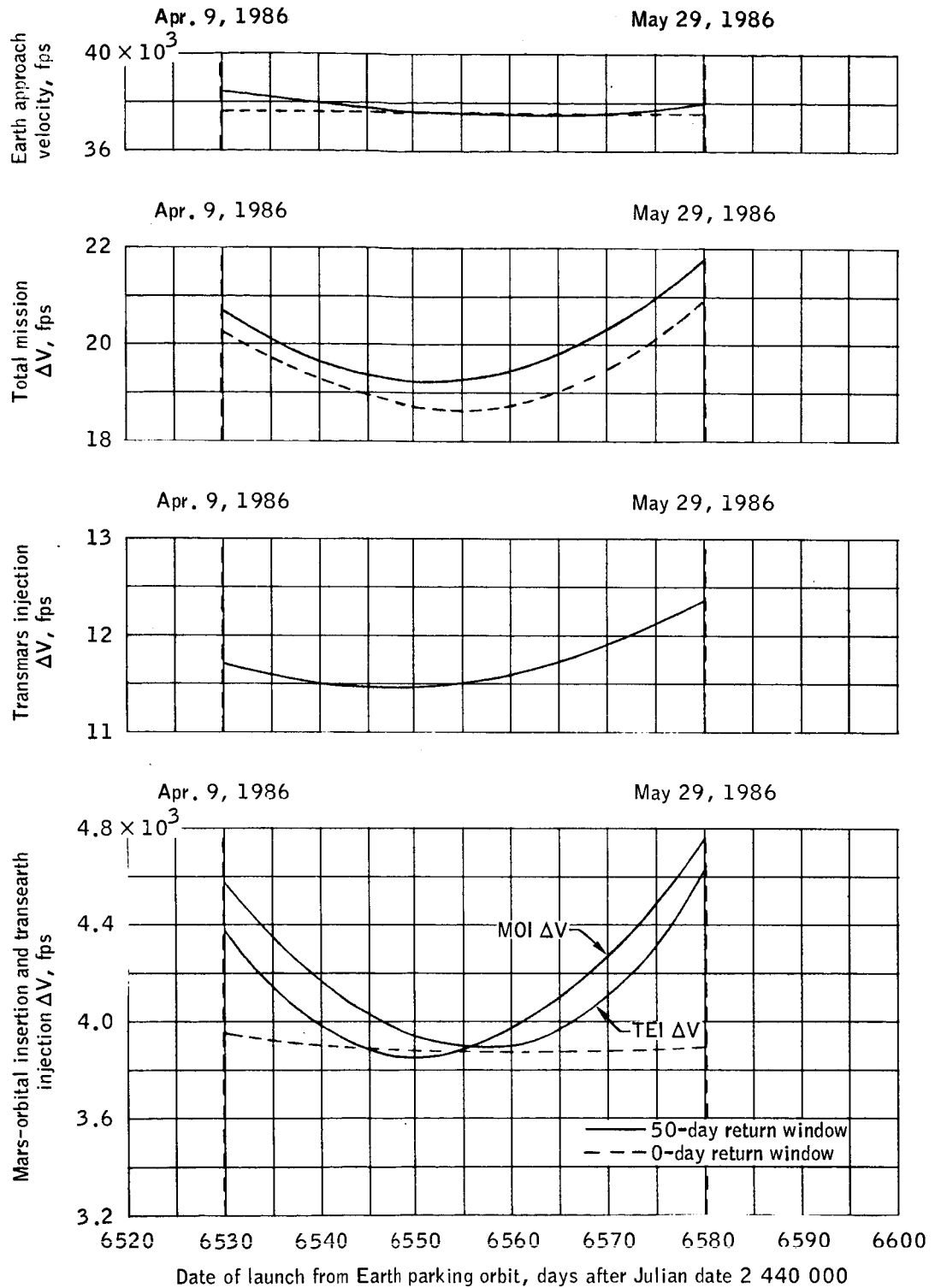
(d) The 1981 mission window.

Figure 3.- Continued.



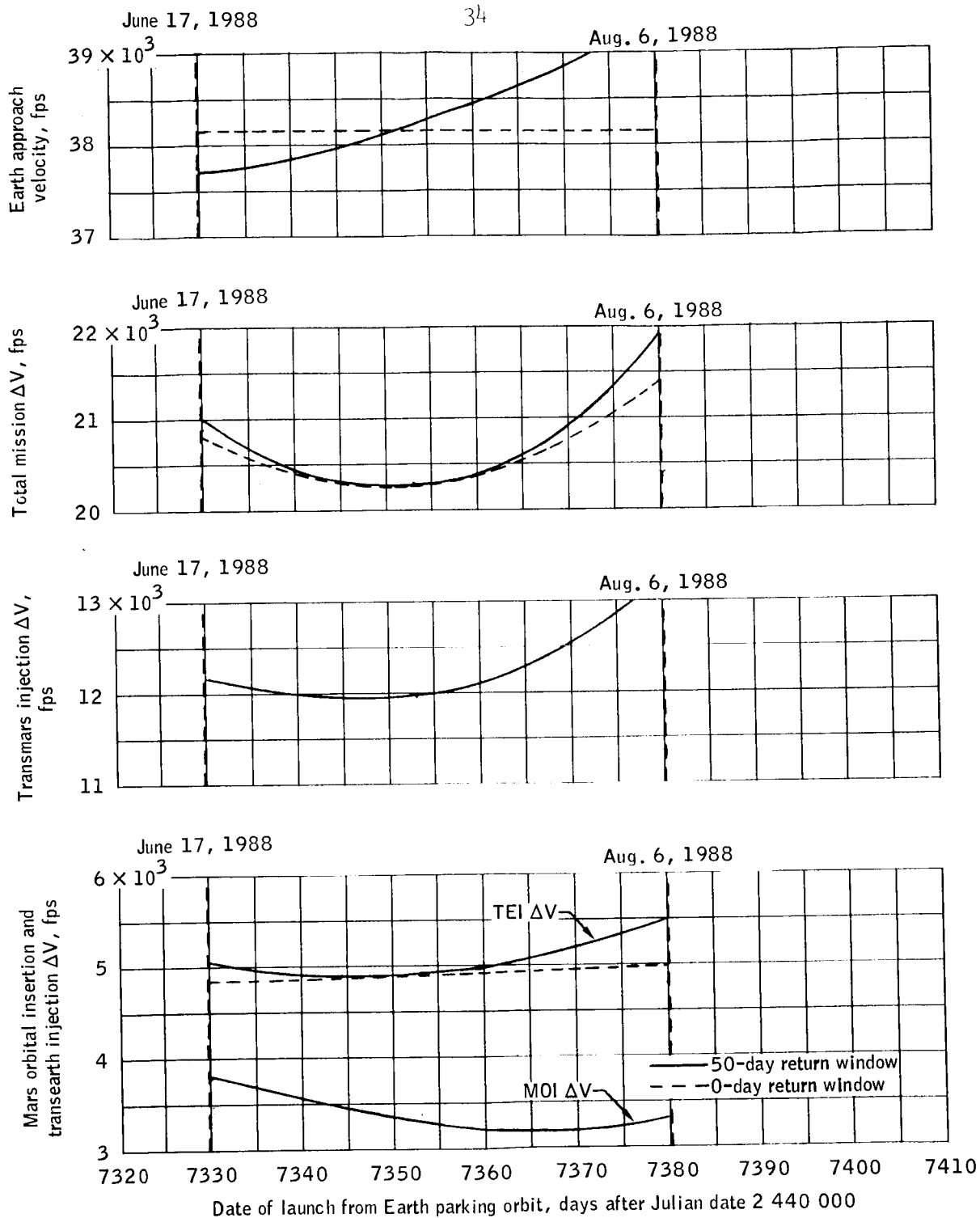
(e) The 1983 mission window.

Figure 3.- Continued.



(f) The 1986 mission window.

Figure 3.- Continued.



(g) The 1988 mission window.

Figure 3.- Concluded.

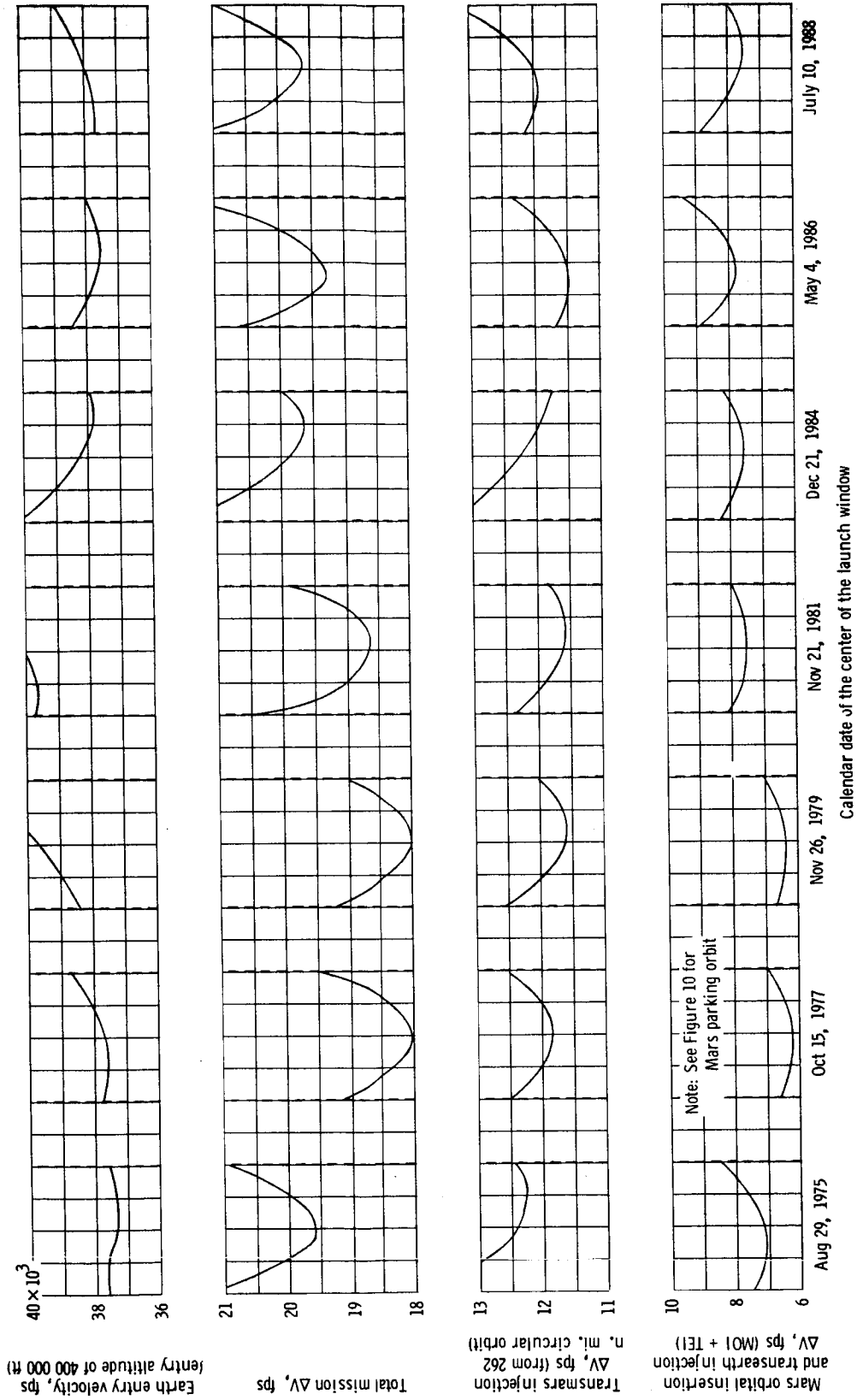


Figure 4. - Variation of mission velocity requirements during the Earth-orbital launch window for minimum ΔV Mars orbital missions between 1975 and 1990.

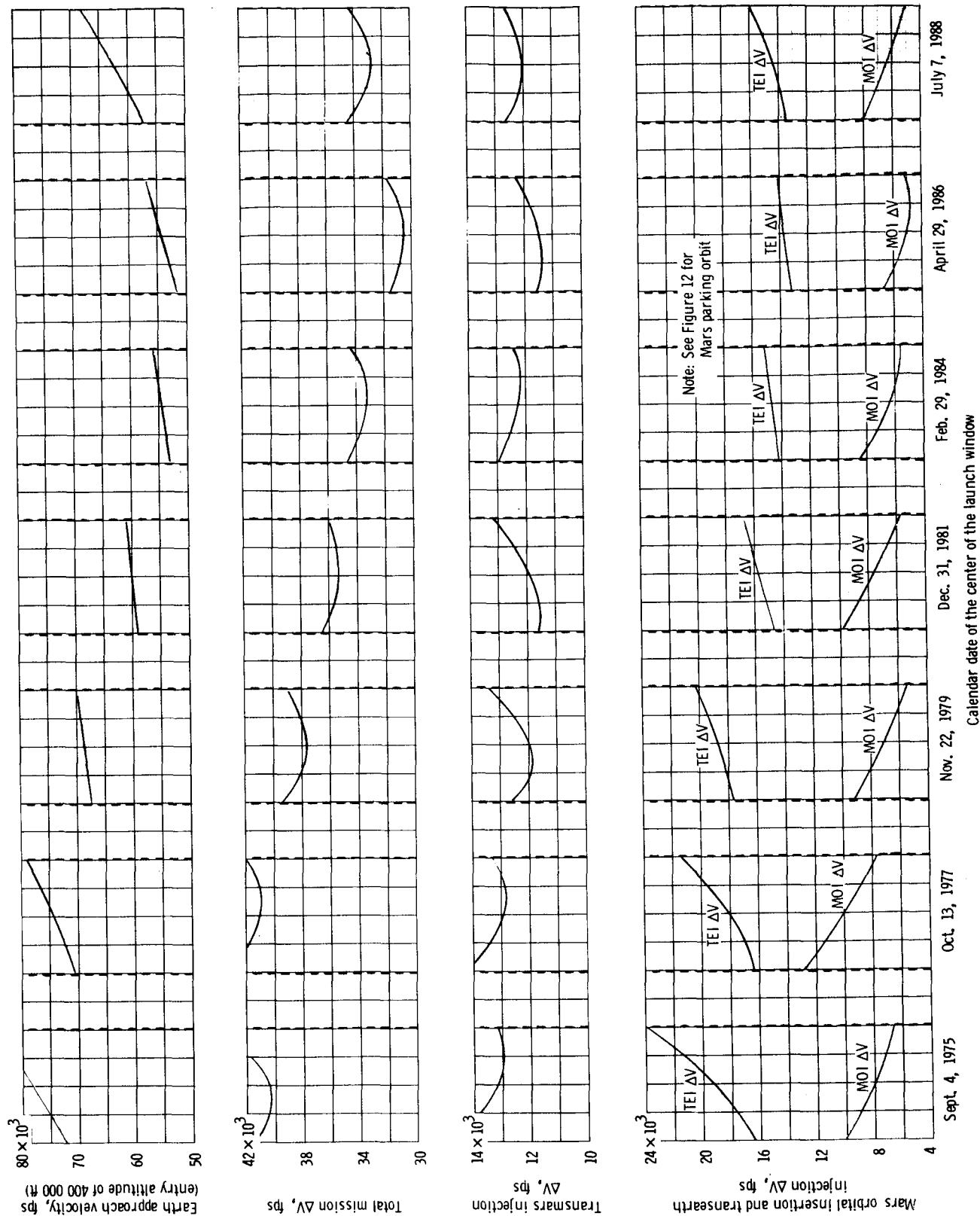
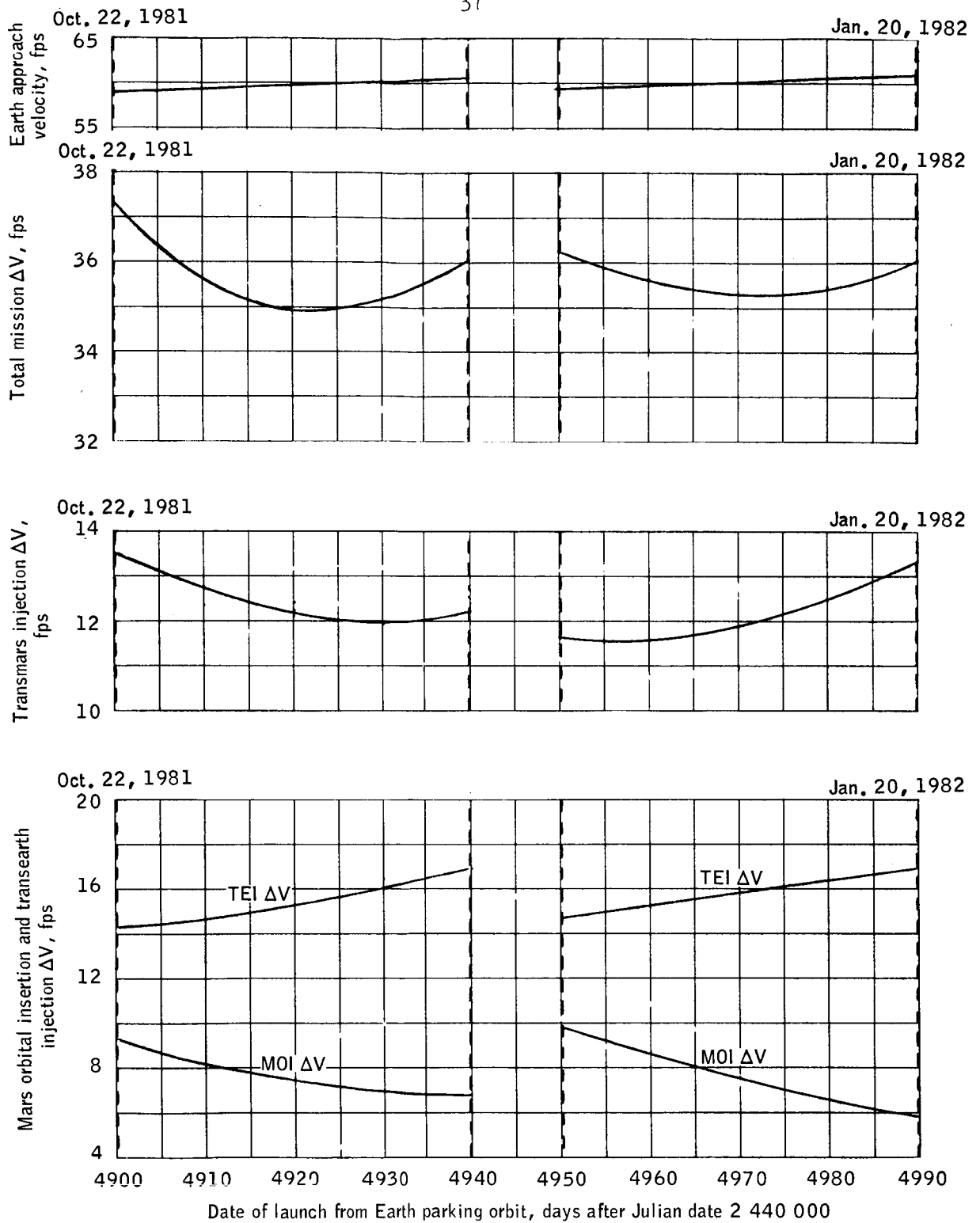
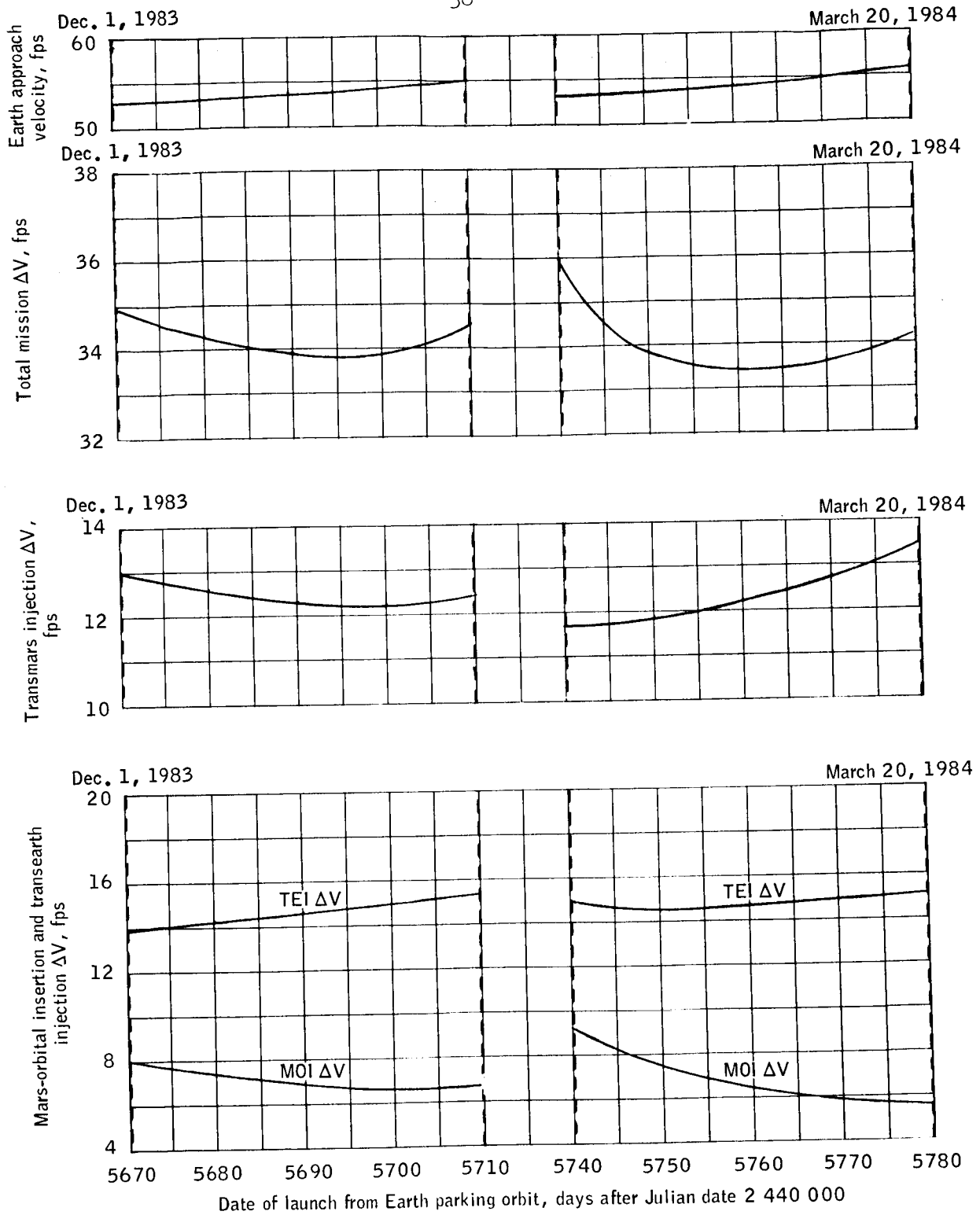


Figure 5. - Variation of mission velocity requirements during the Earth-orbital launch window for short stay time Mars orbital missions between 1975 and 1990.



(a) 1981 mission window.

Figure 6.- The variation of mission velocity requirements for the short stay time missions.



(b) 1983 and 1984 mission windows.

Figure 6.- Concluded.

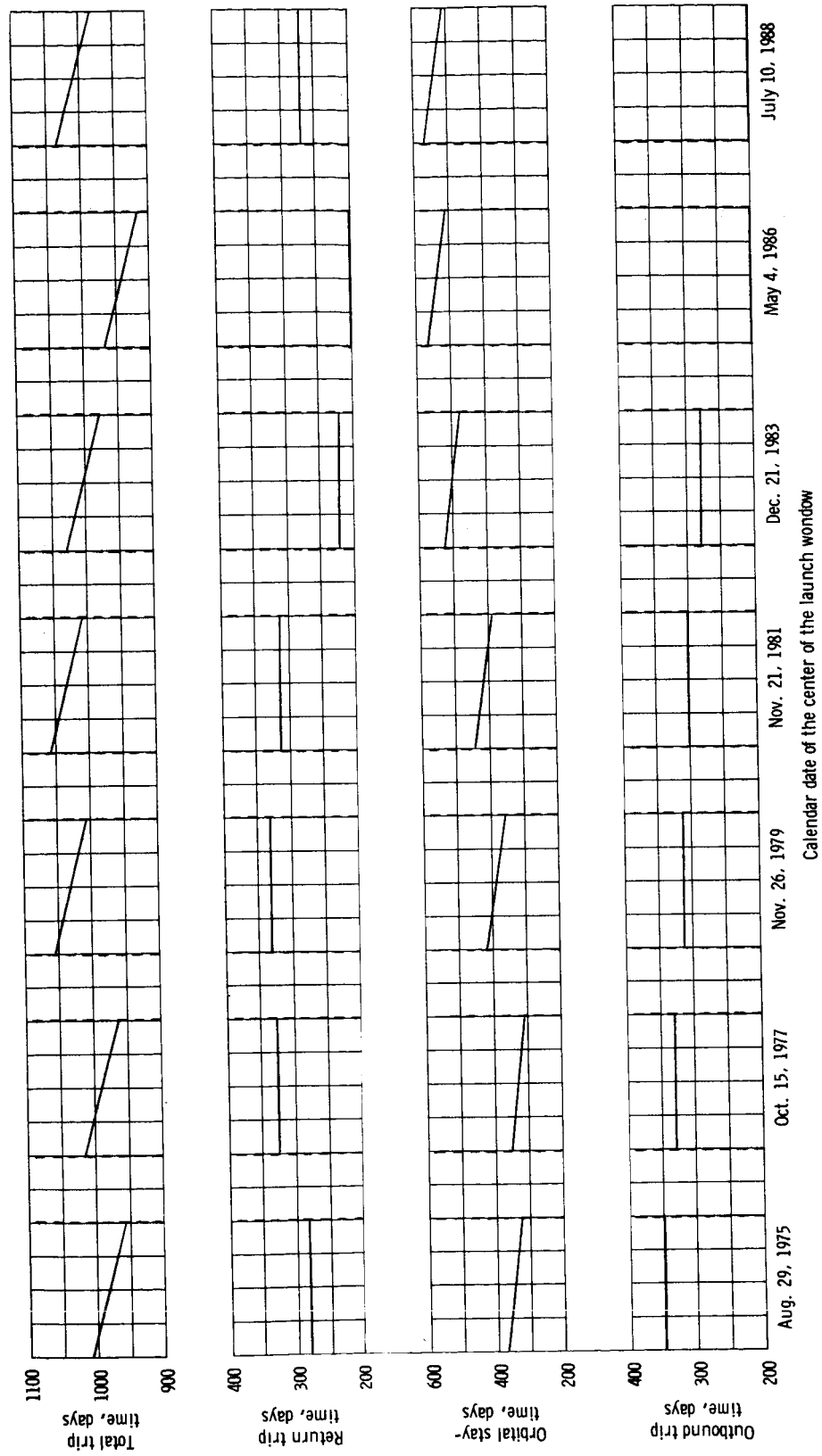


Figure 7. - Variation of trip times during the mission launch window for the minimum ΔV Mars orbital missions between 1975 and 1988.

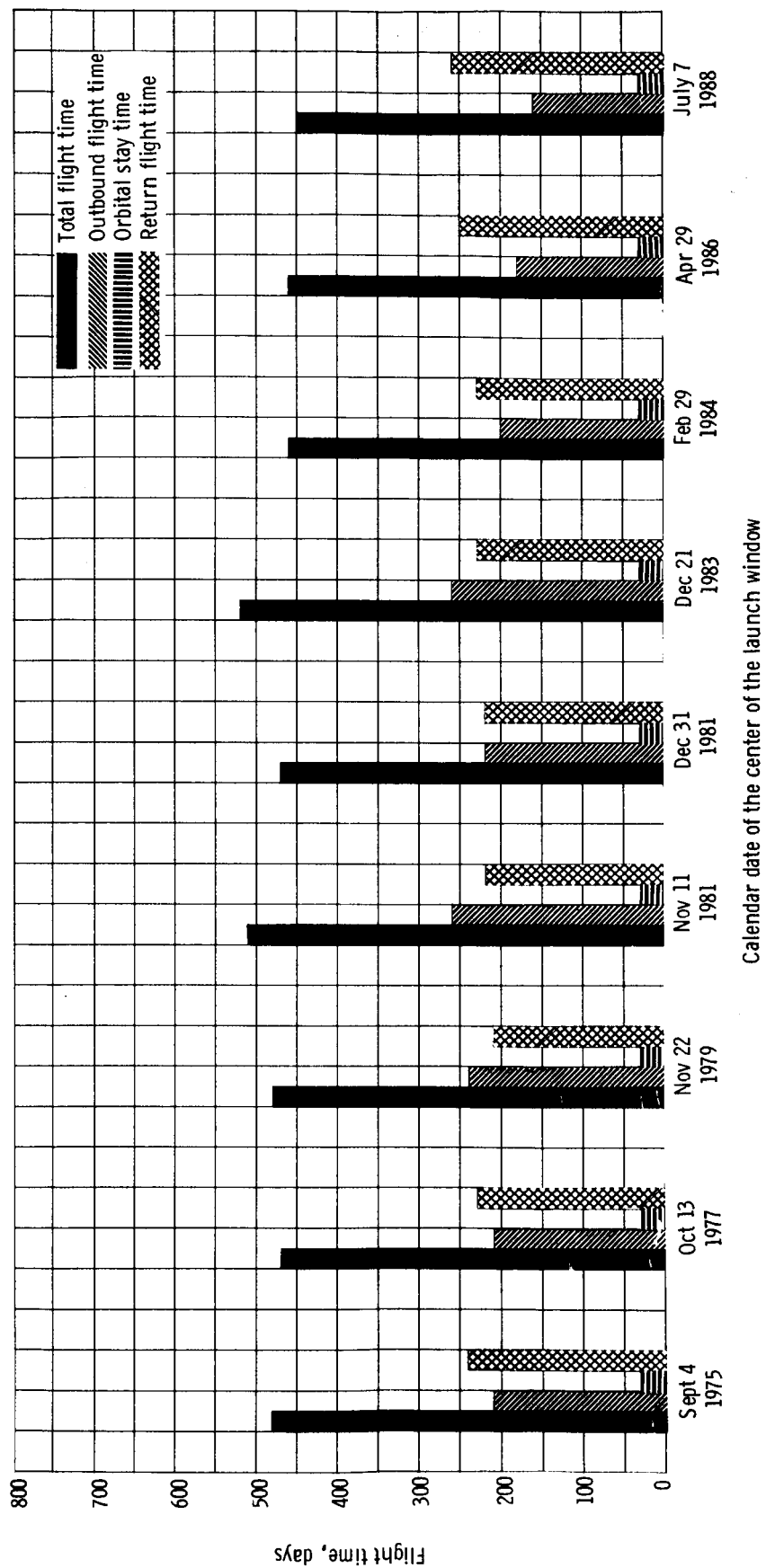


Figure 8. - Launch dates and trip times for short stay time missions between 1975 and 1988.

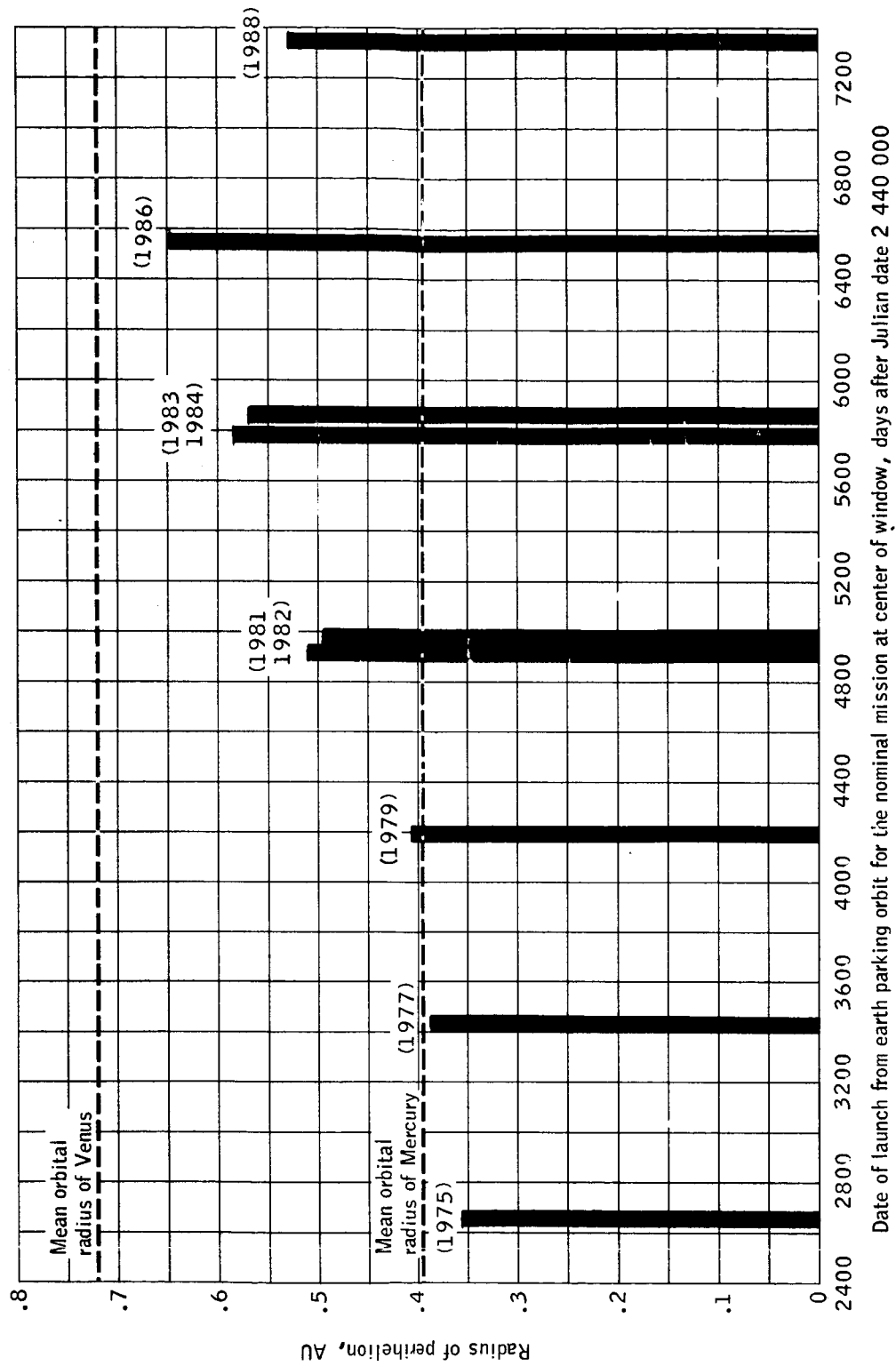
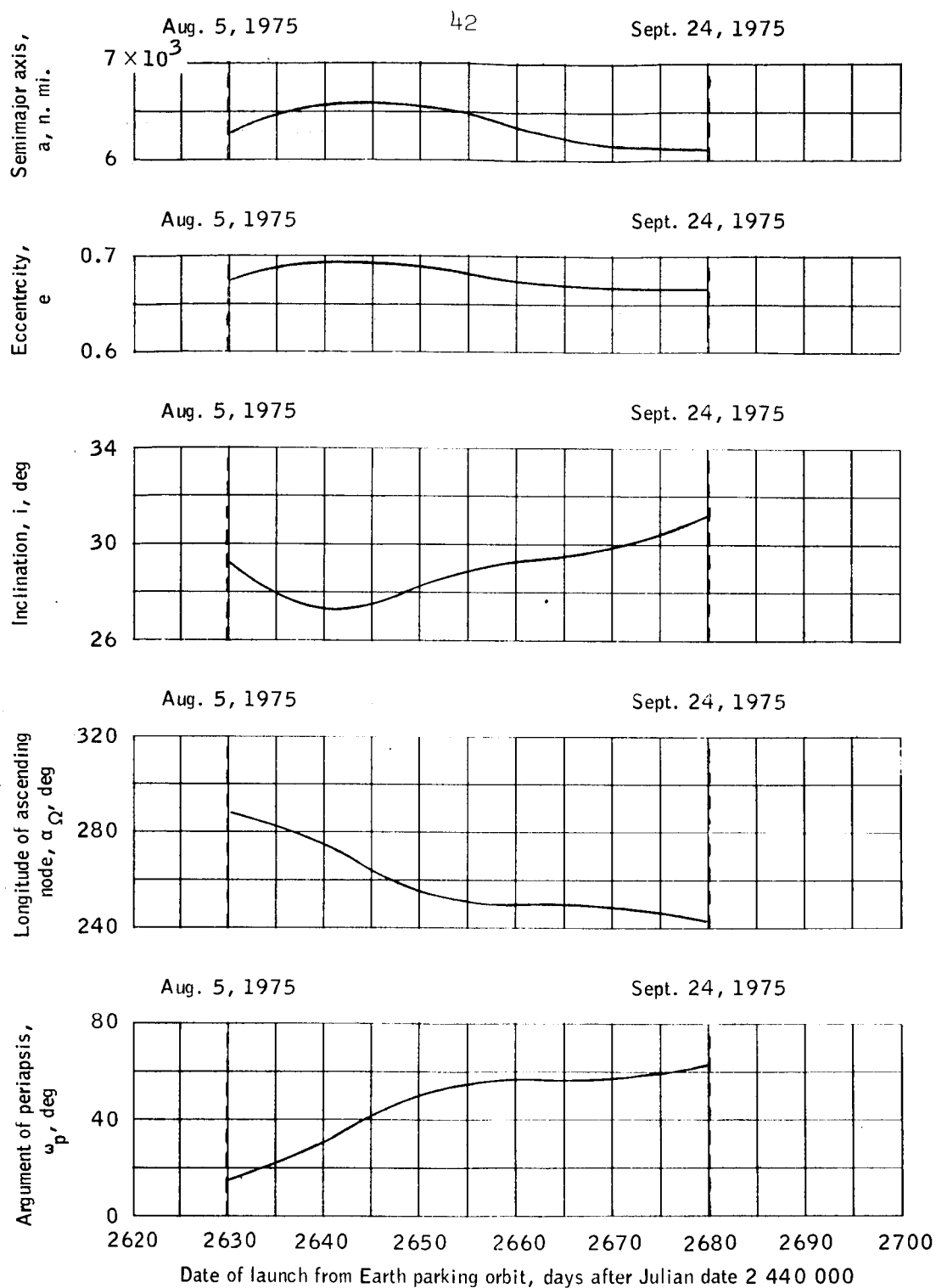
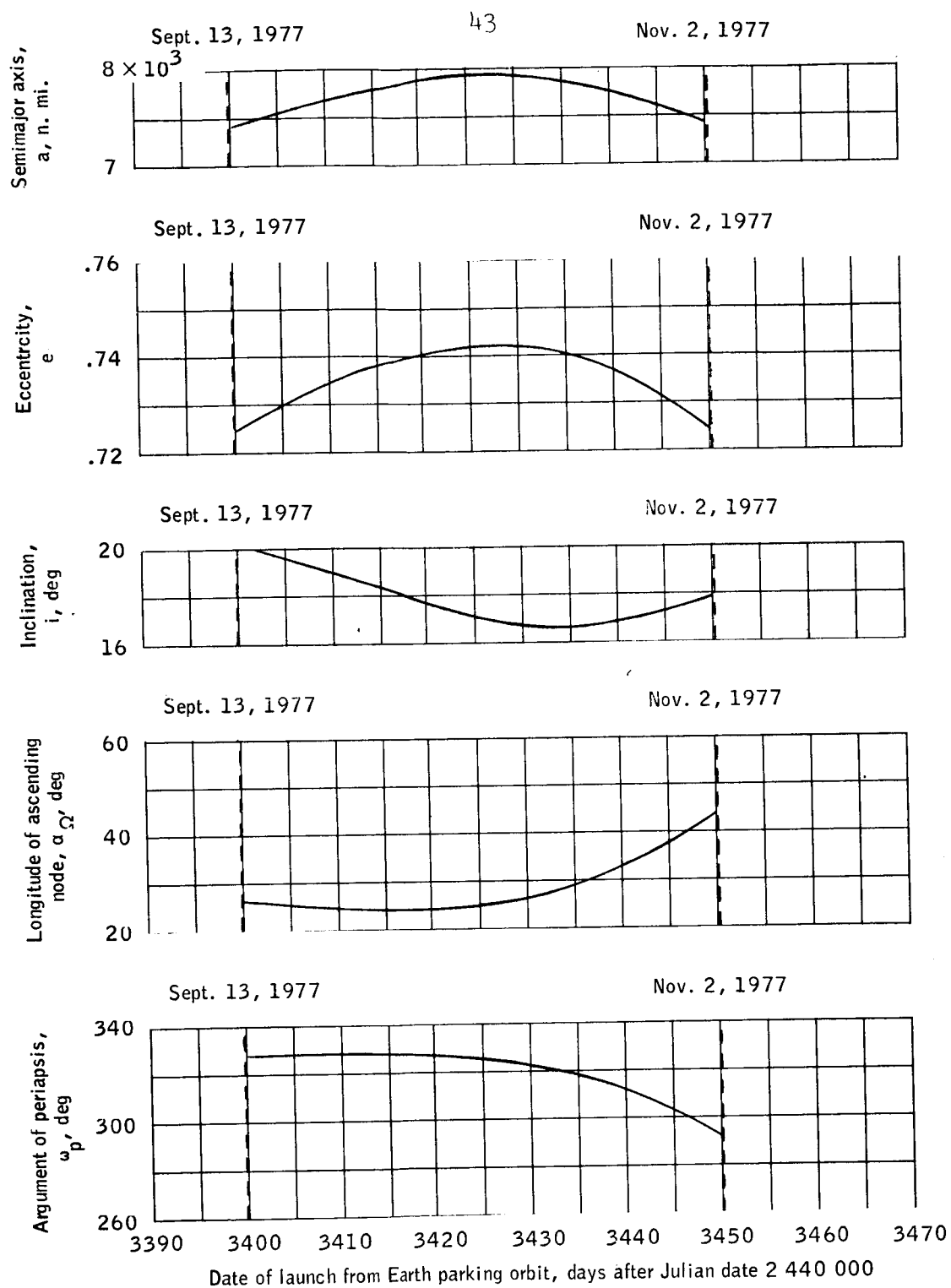


Figure 9.- The perihelion distance of the return trajectory for short stay time missions between 1975 and 1988.



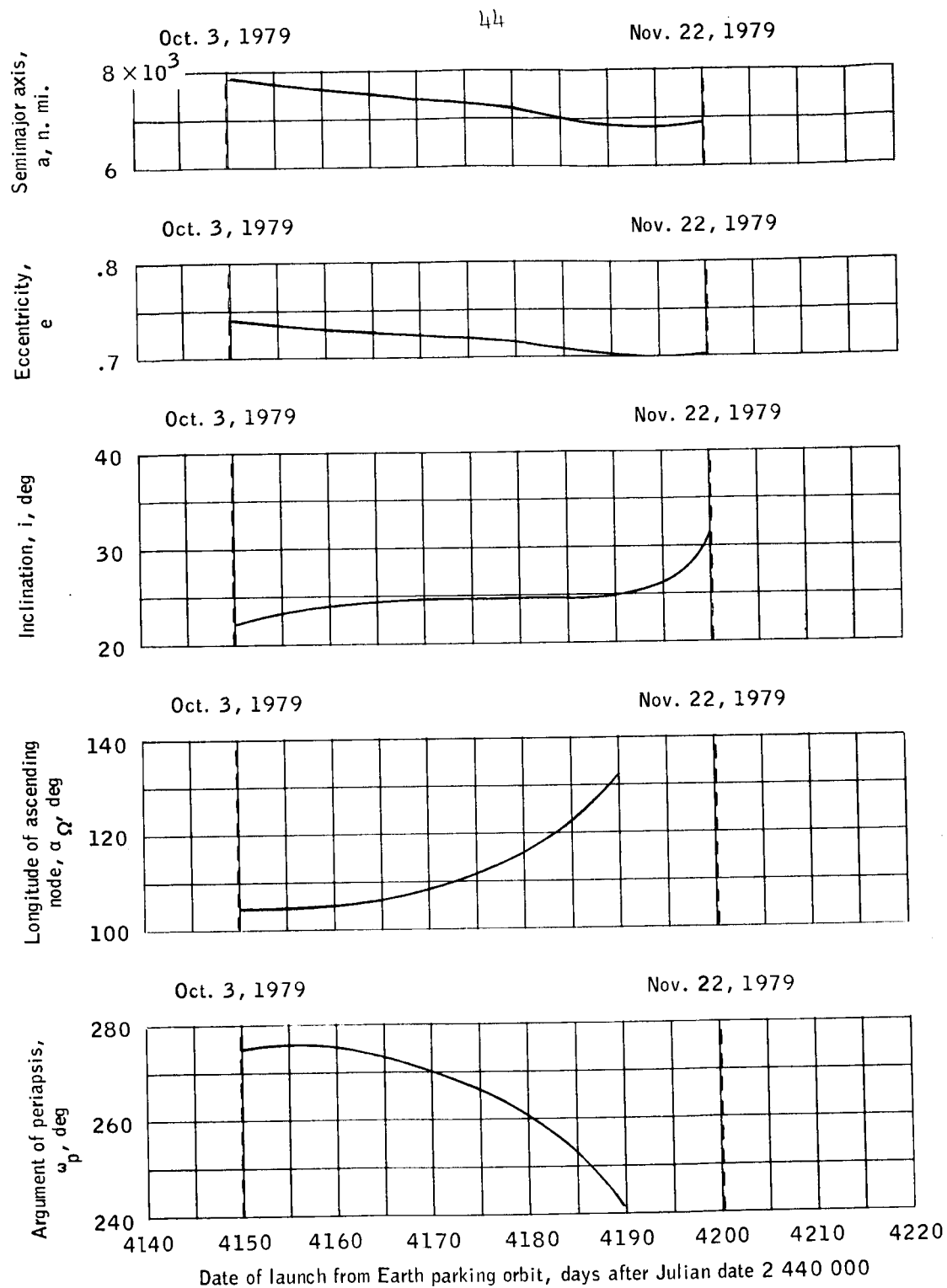
(a) The 1975 mission window.

Figure 10.- The orbital elements of the parking orbit for minimum ΔV missions.



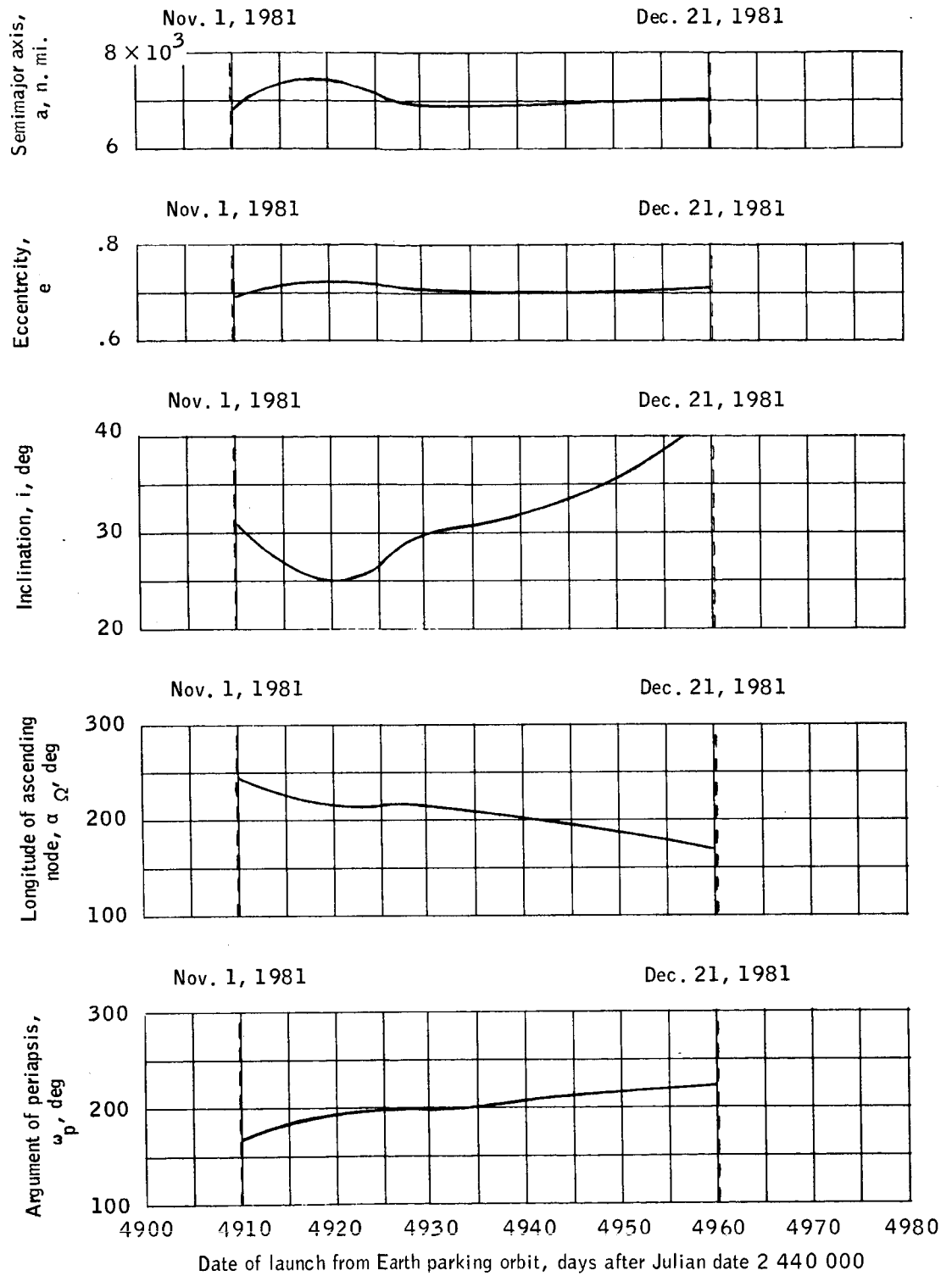
(b) The 1977 mission window.

Figure 10.- Continued.



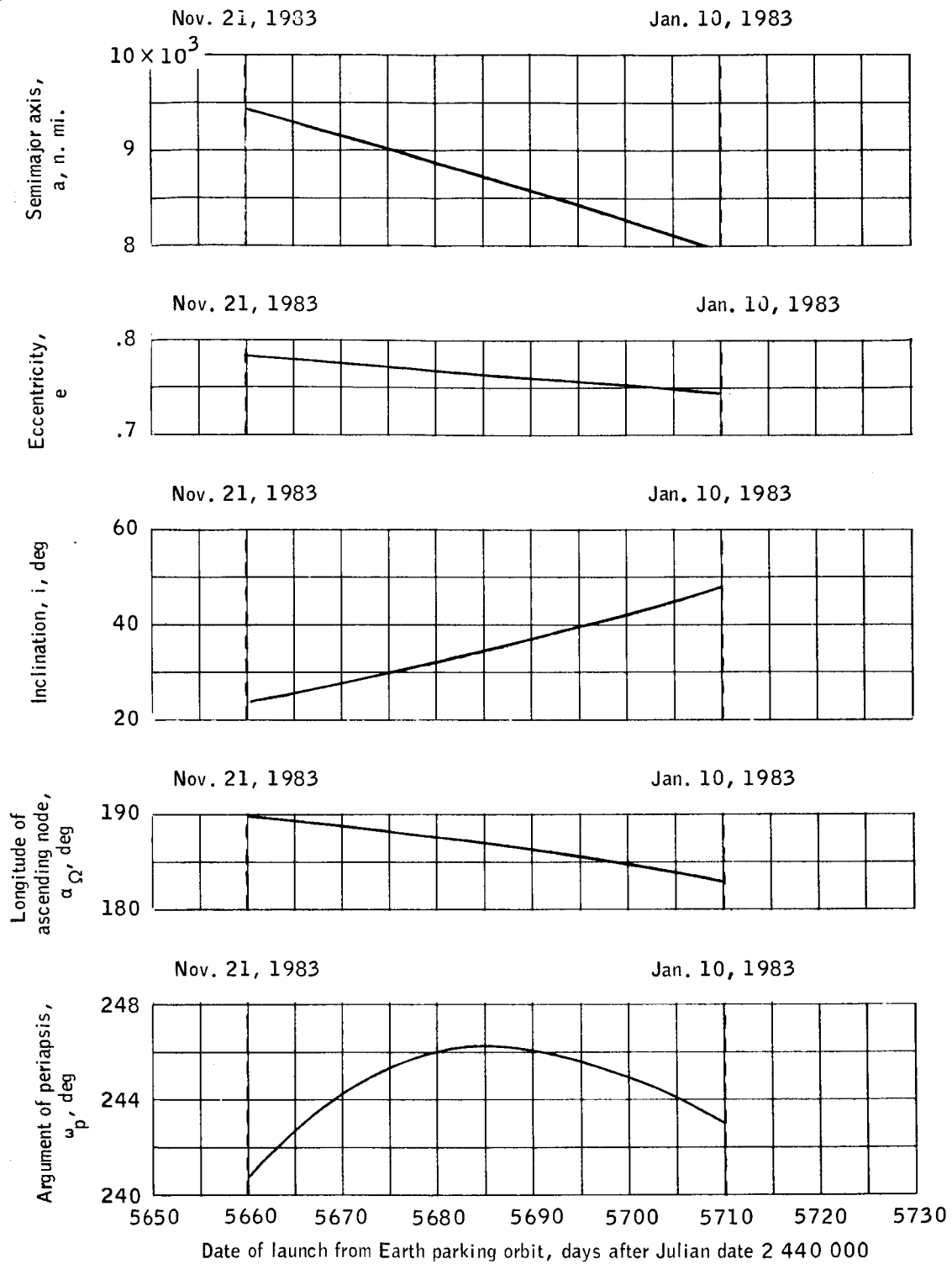
(c) The 1979 mission window.

Figure 10.- Continued.



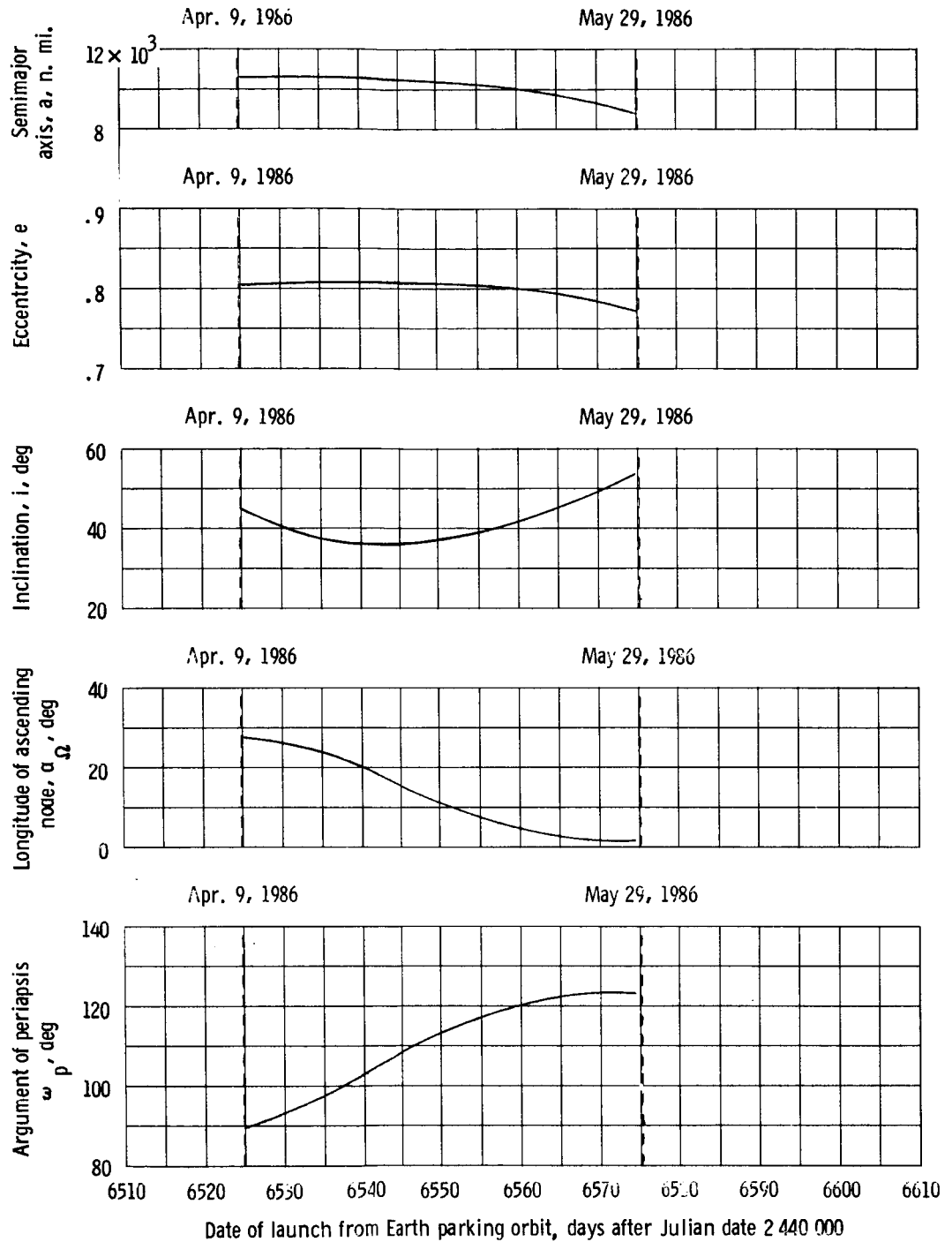
(d) The 1981 mission window.

Figure 10.- Continued.



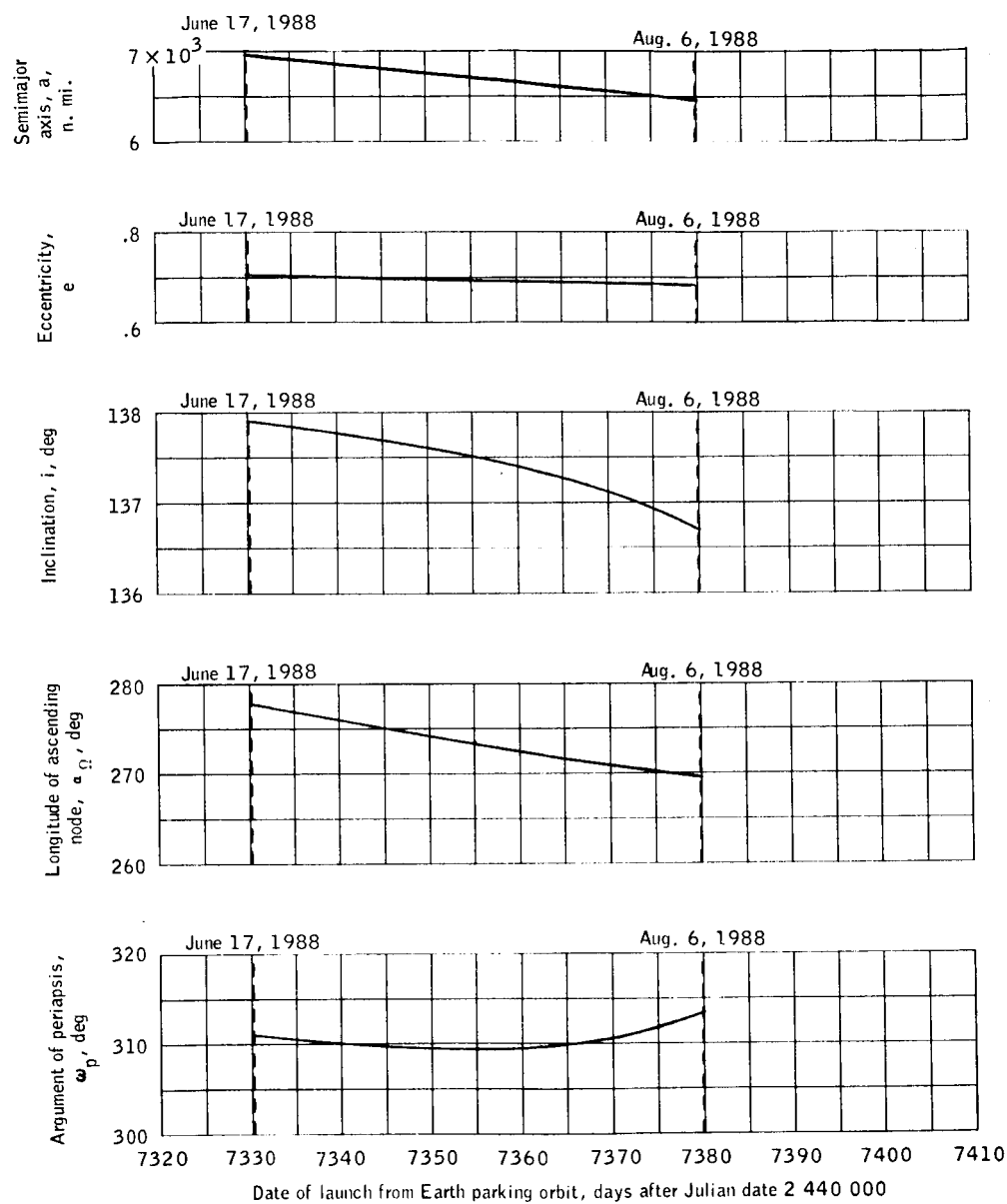
(e) The 1983 mission window.

Figure 10.- Continued.



(f) The 1986 mission window.

Figure 10. - Continued.



(g) The 1988 mission window.

Figure 10.- Concluded.

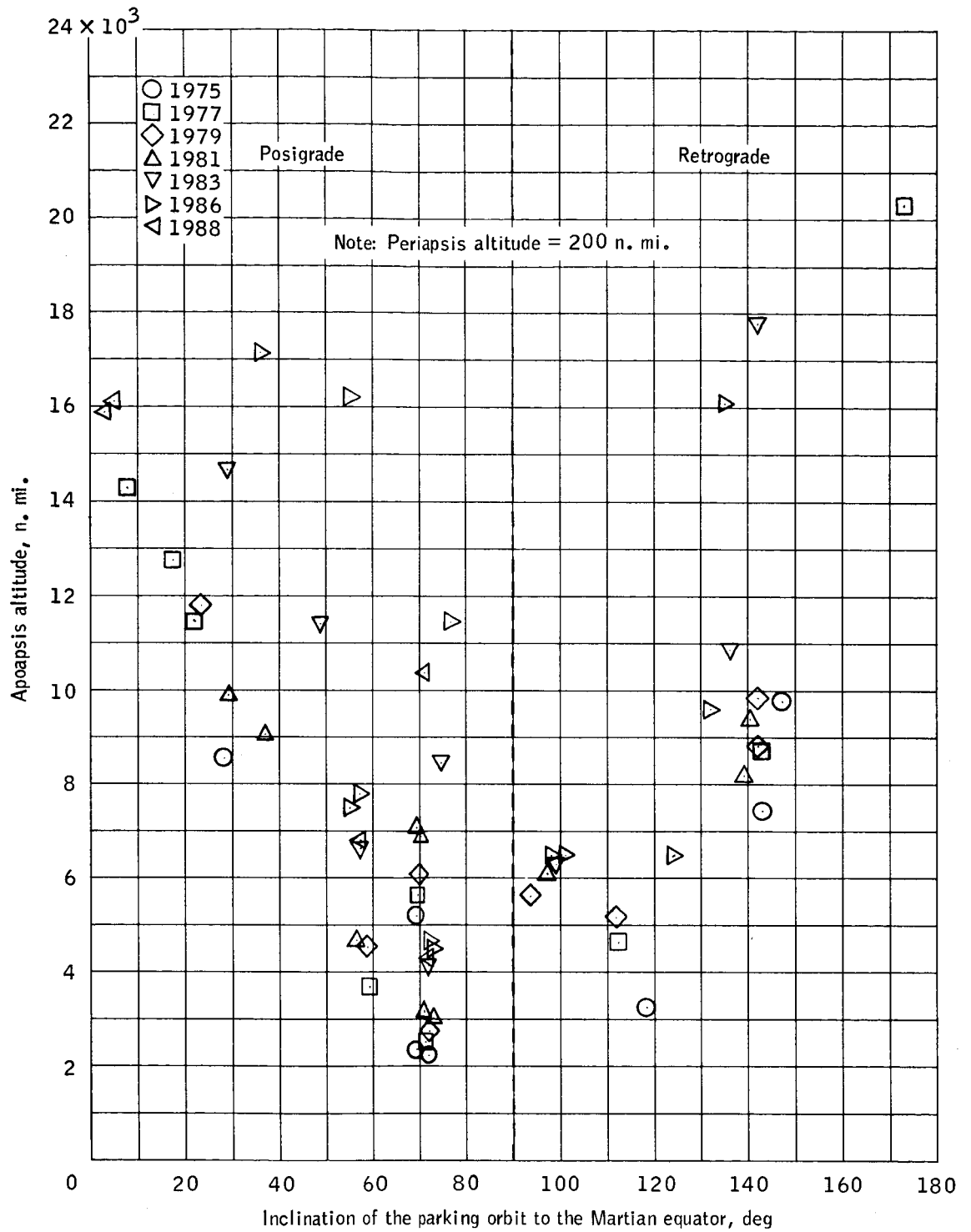
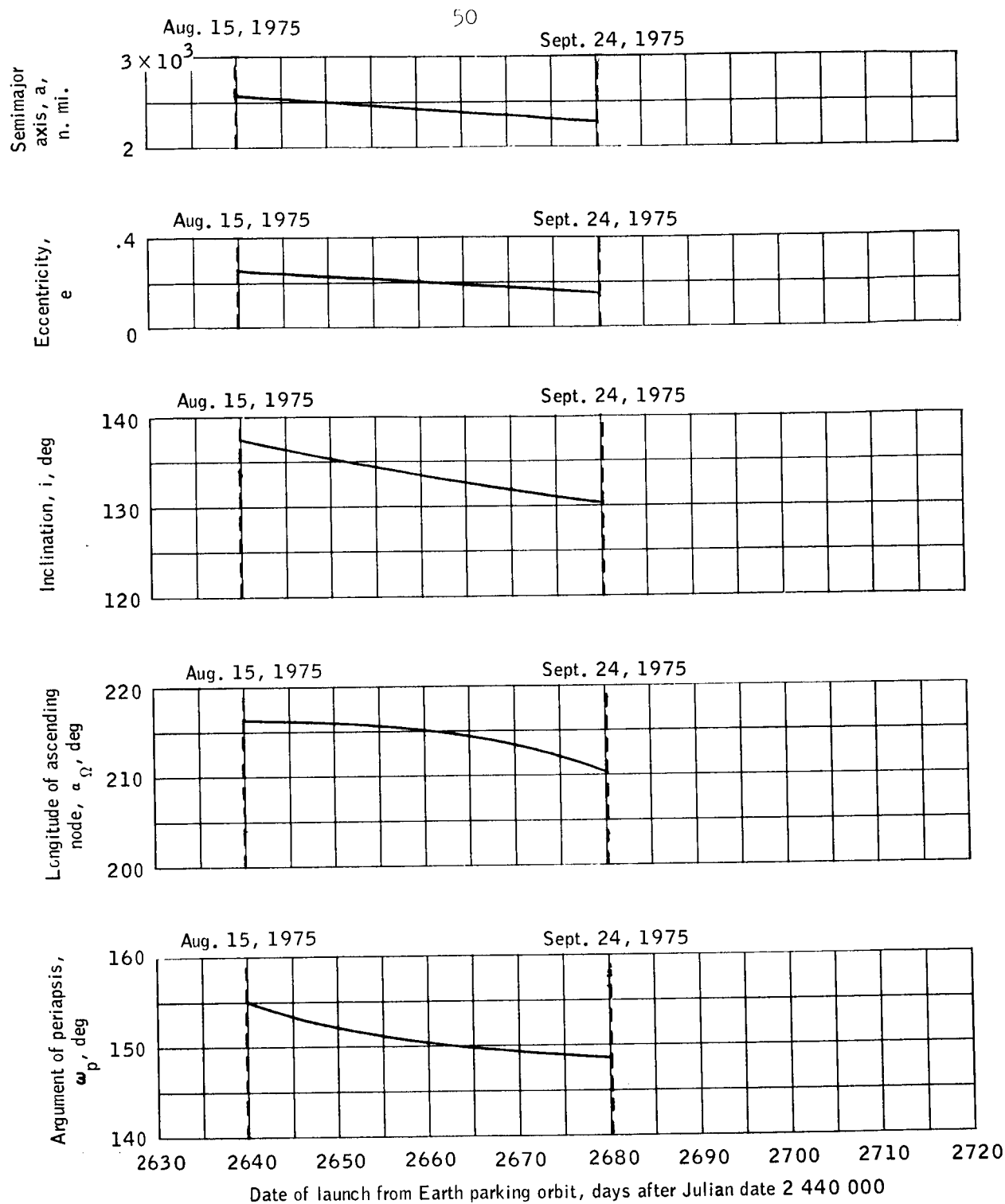
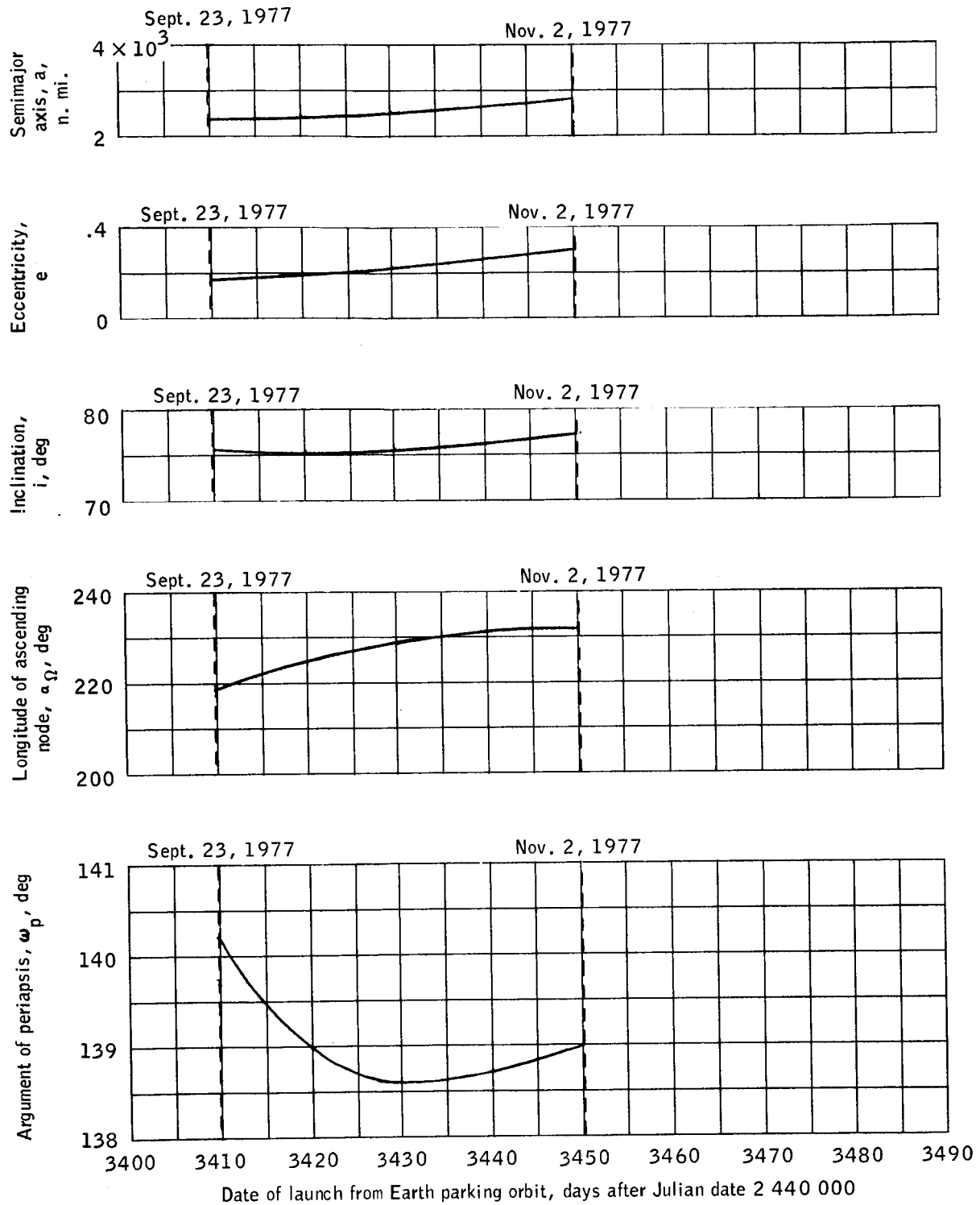


Figure 11.- The range of apoapsis altitudes and orbital inclinations which occur during the minimum ΔV missions between 1975 and 1988.



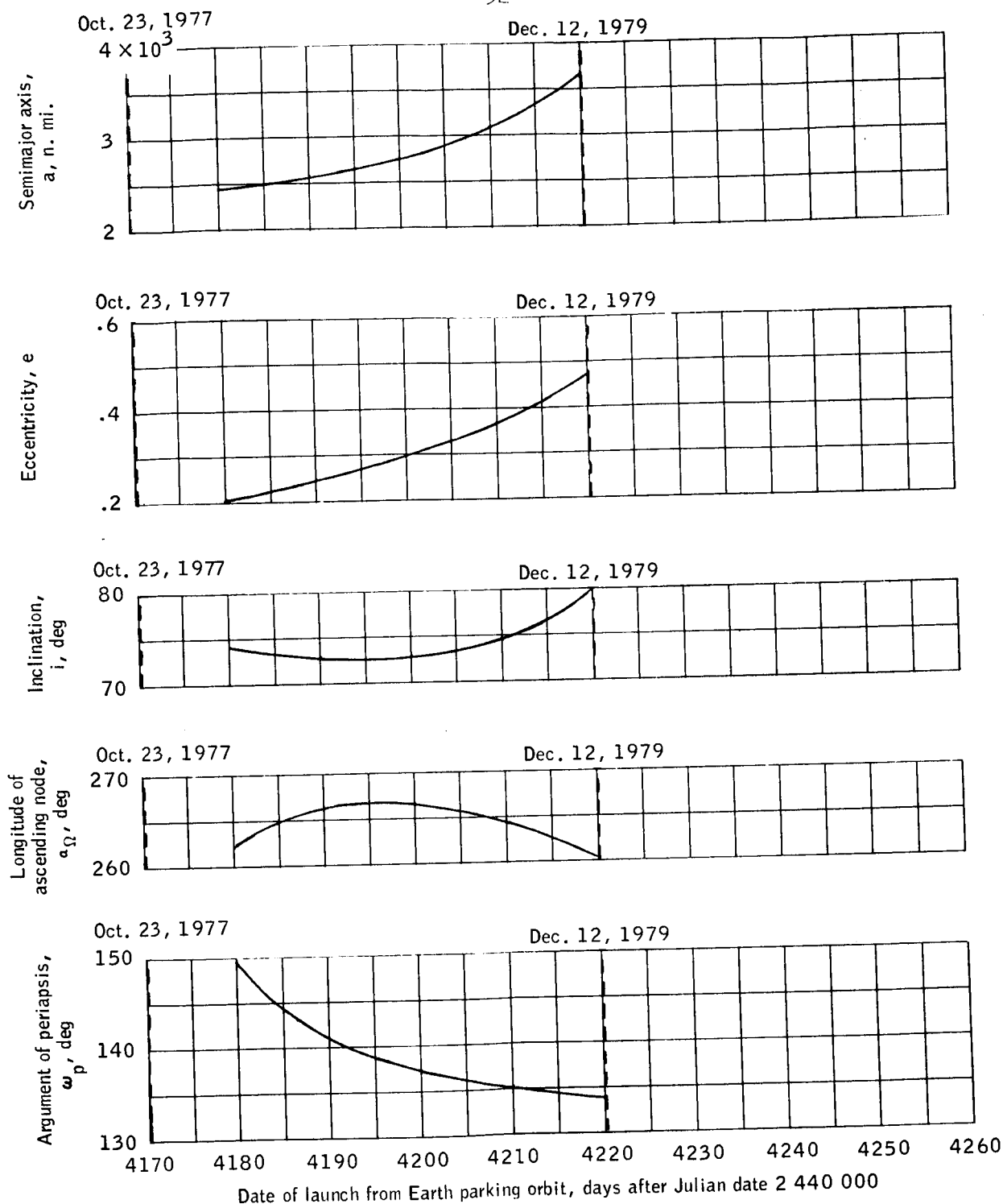
(a) The 1975 mission window.

Figure 12.- The orbital elements of the parking orbit for the short stay time missions.



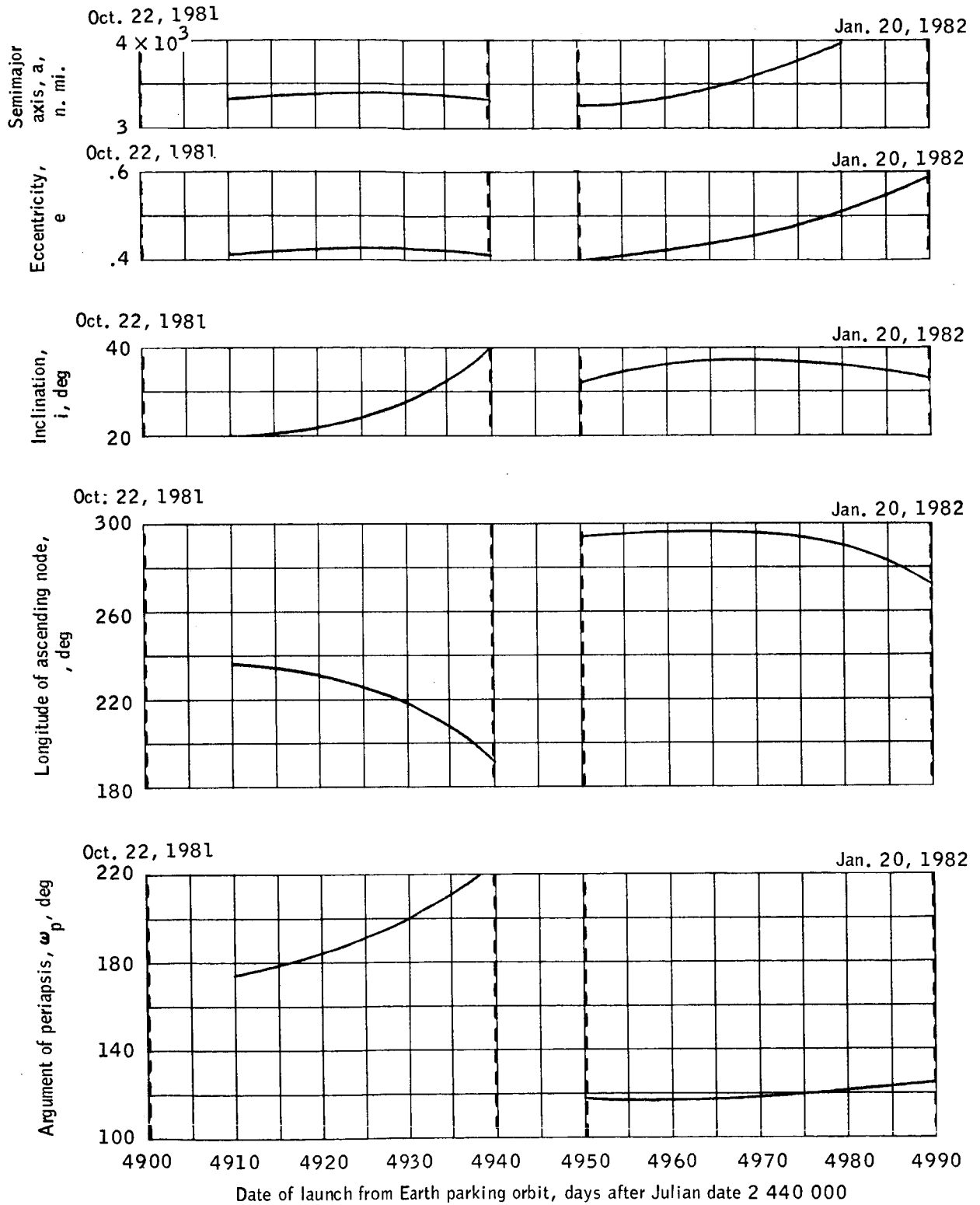
(b) The 1977 mission window.

Figure 12.- Continued.



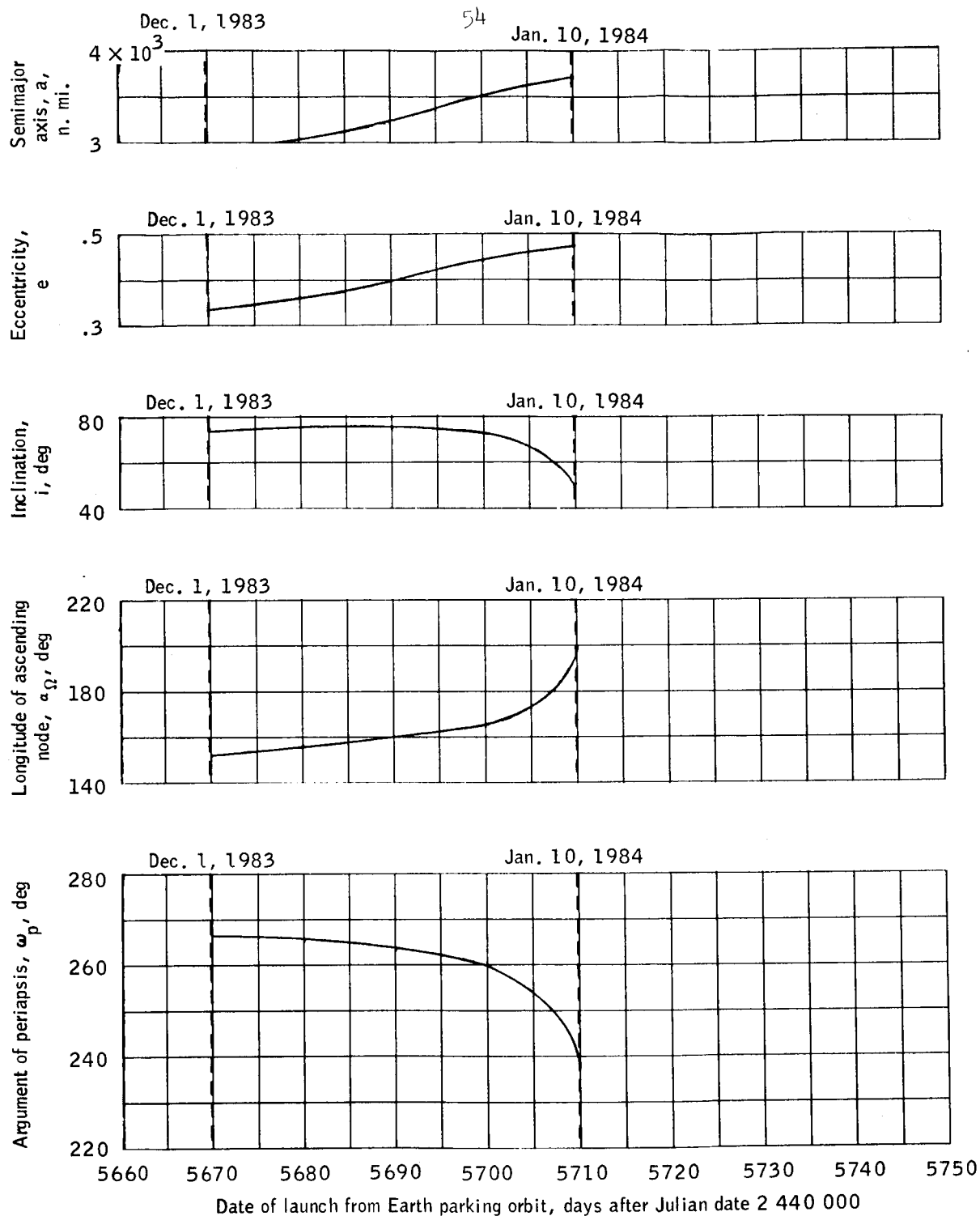
(c) The 1979 mission window.

Figure 12.- Continued.



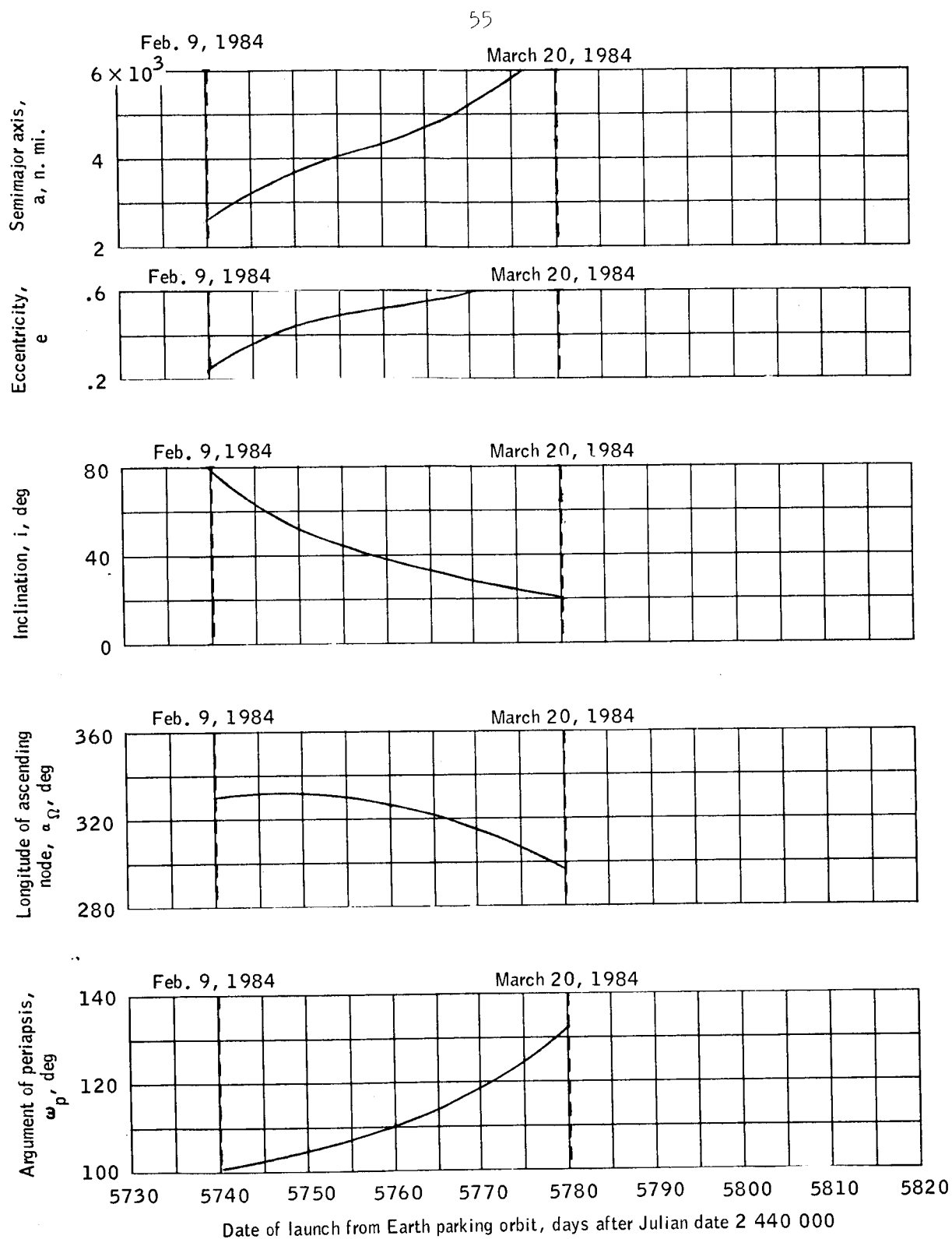
(d) The 1981 mission window.

Figure 12.- Continued.



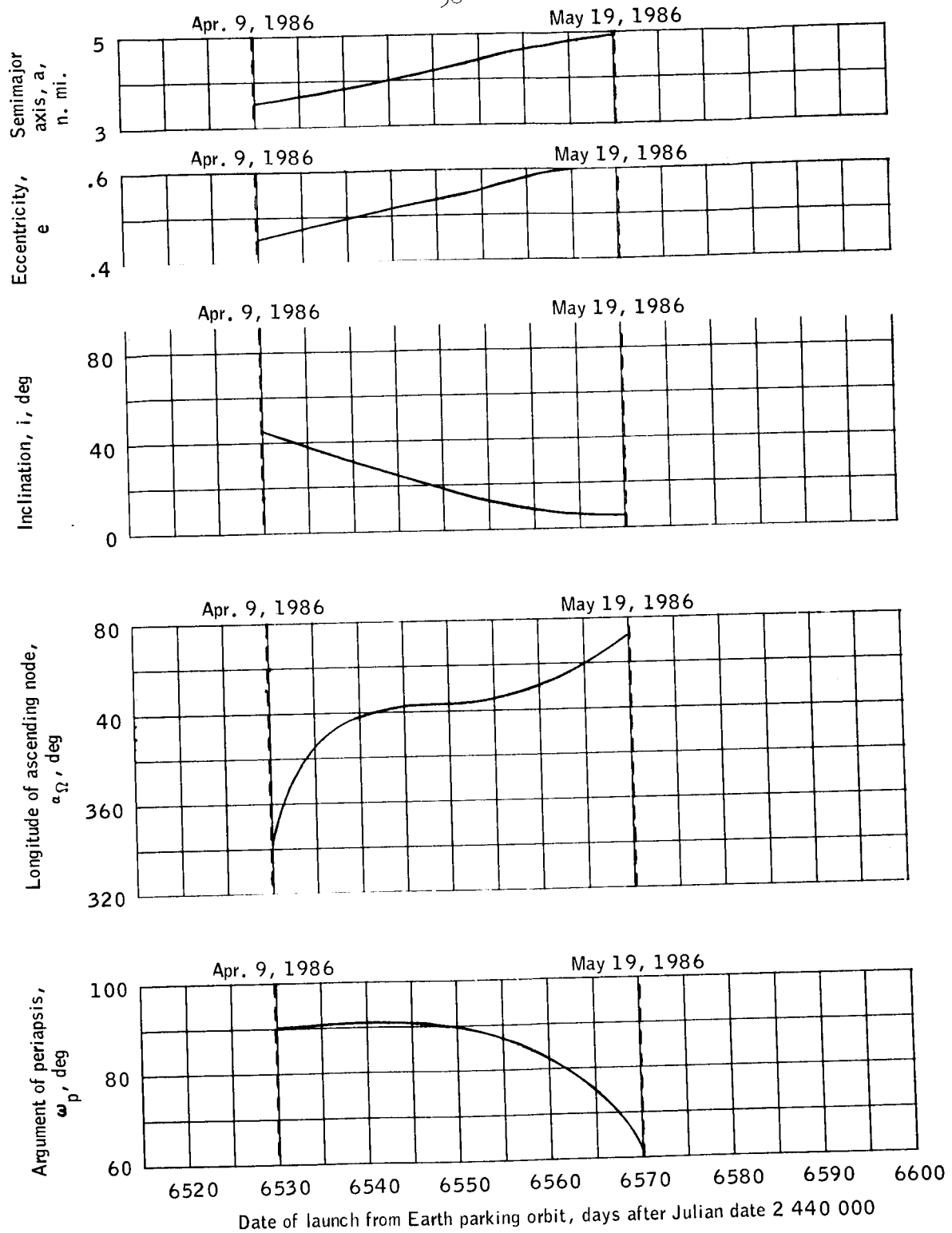
(e) The 1983 mission window.

Figure 12.- Continued.



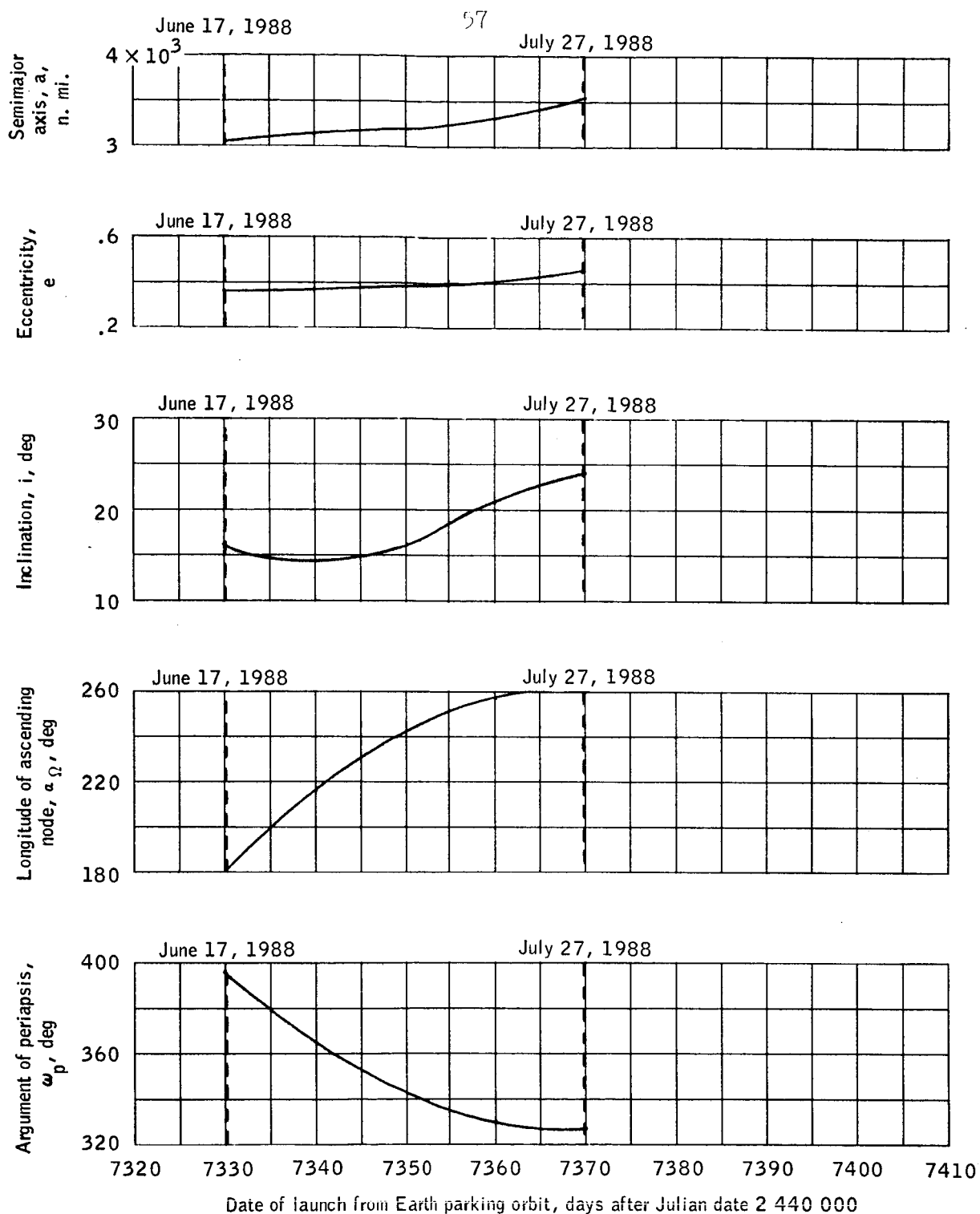
(f) The 1984 mission window.

Figure 12.- Continued.



(g) The 1986 mission window.

Figure 12.- Concluded.



(h) The 1988 mission window.

Figure 12.- Concluded.

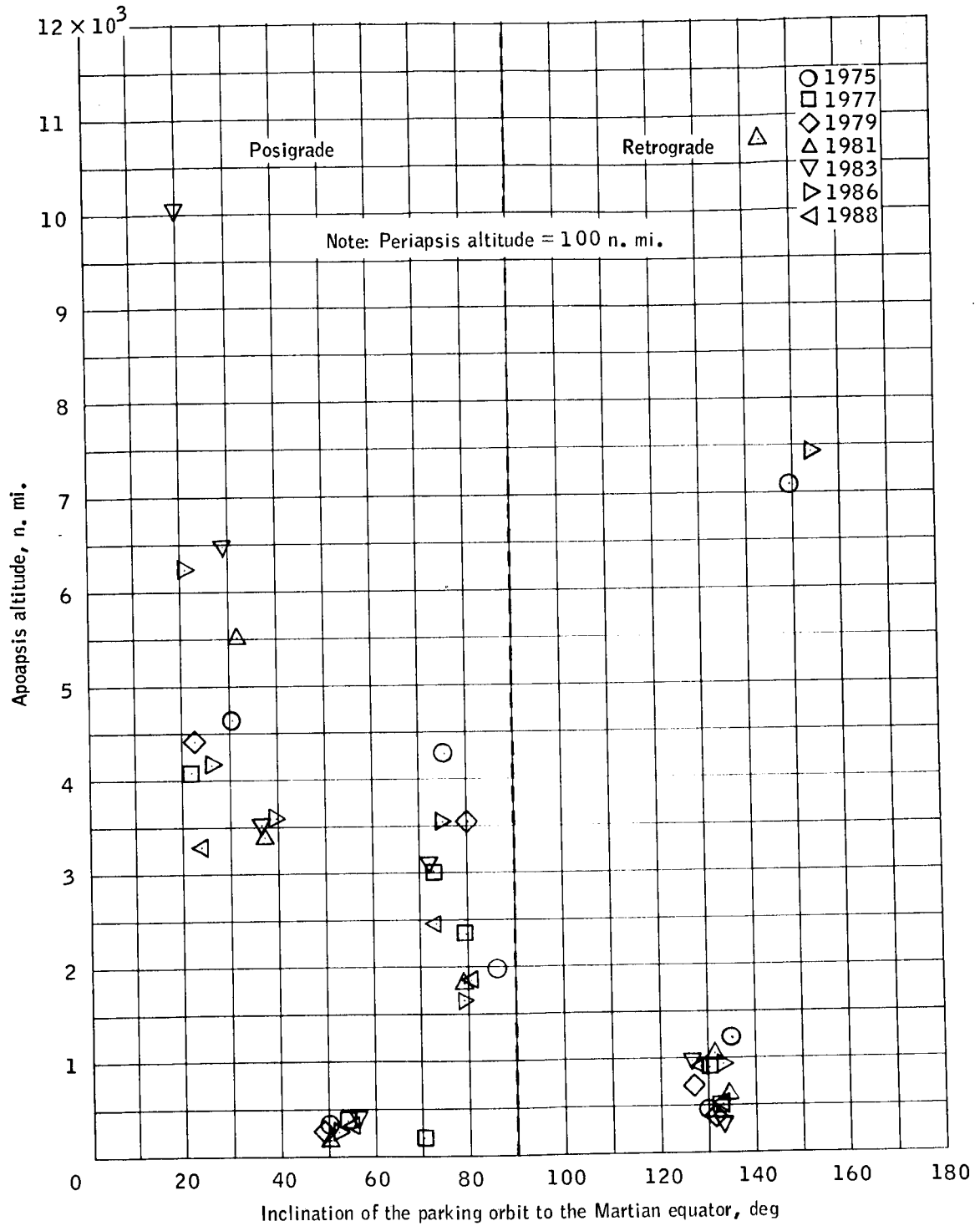


Figure 13.- The range of apoapsis altitudes and orbital inclinations which occur during short stay time missions between 1975 and 1988.

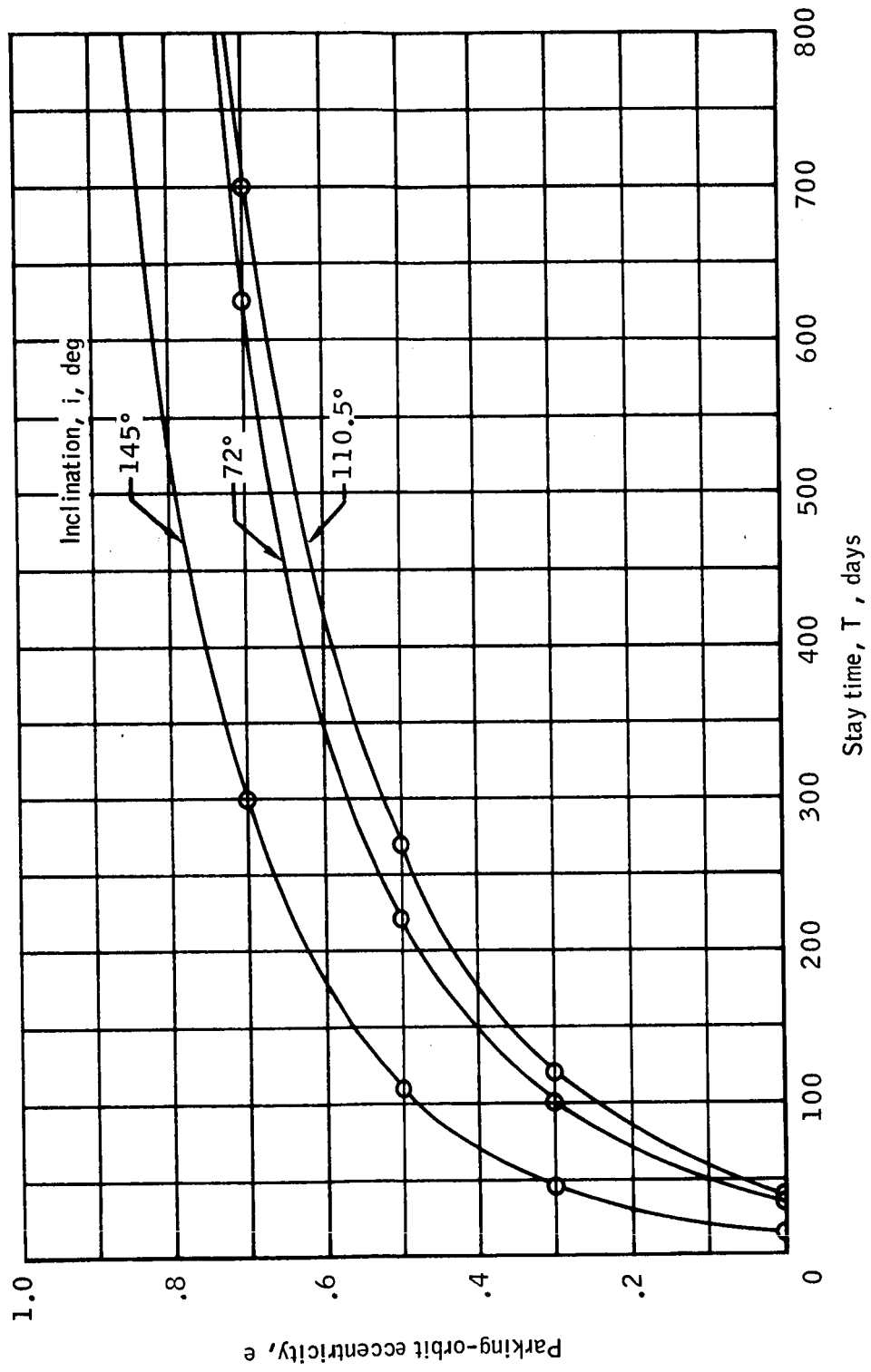


Figure 14.- Variation of orbital eccentricity with stay time for a stationary V_{∞} geometry.

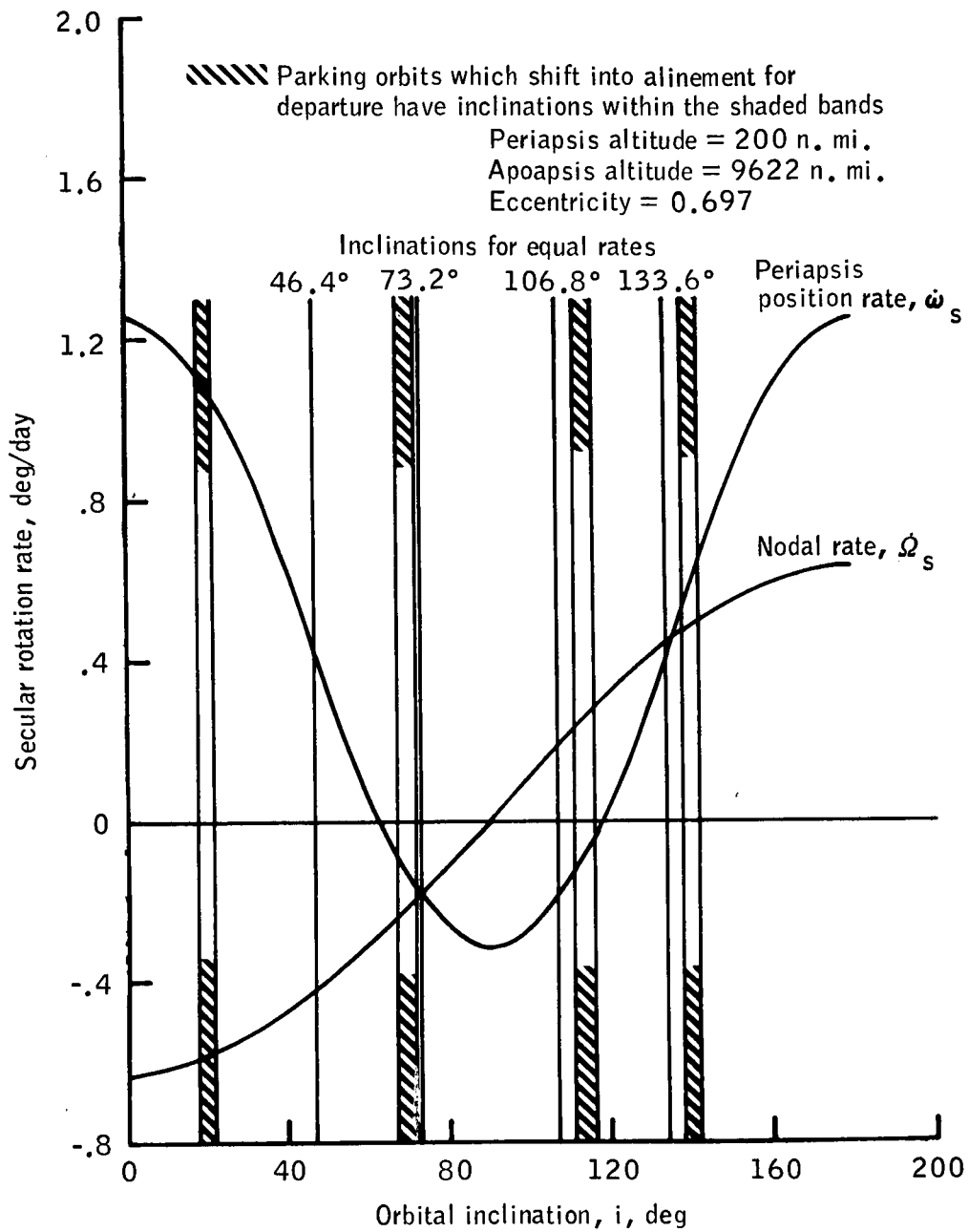


Figure 15.- Secular rotation rates of the parking orbit node and perapsis position vectors due to planetary oblateness.

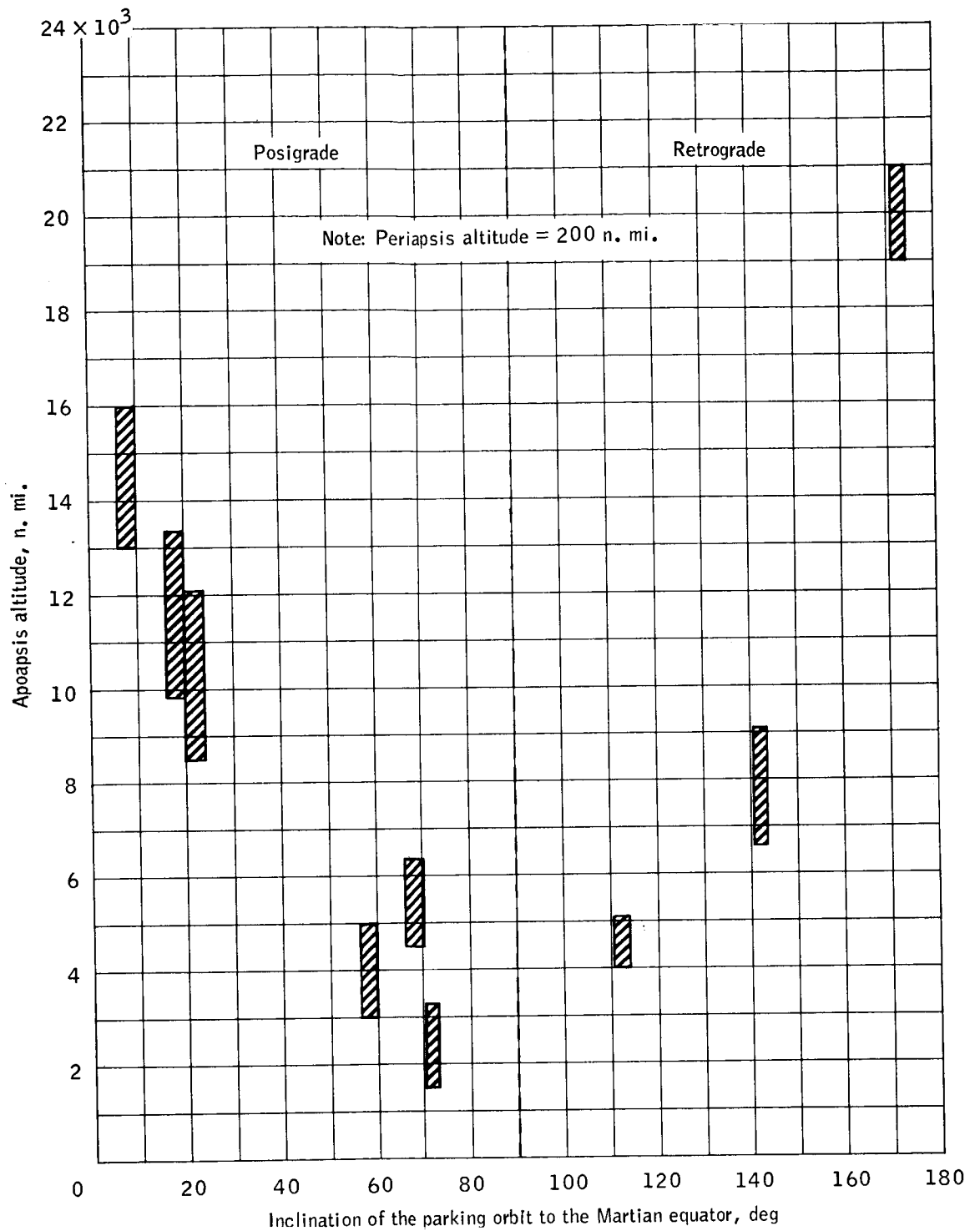


Figure 16.-The correlation of apoapsis altitude and orbital inclination for regressing orbits which occur during a minimum ΔV mission in 1977.

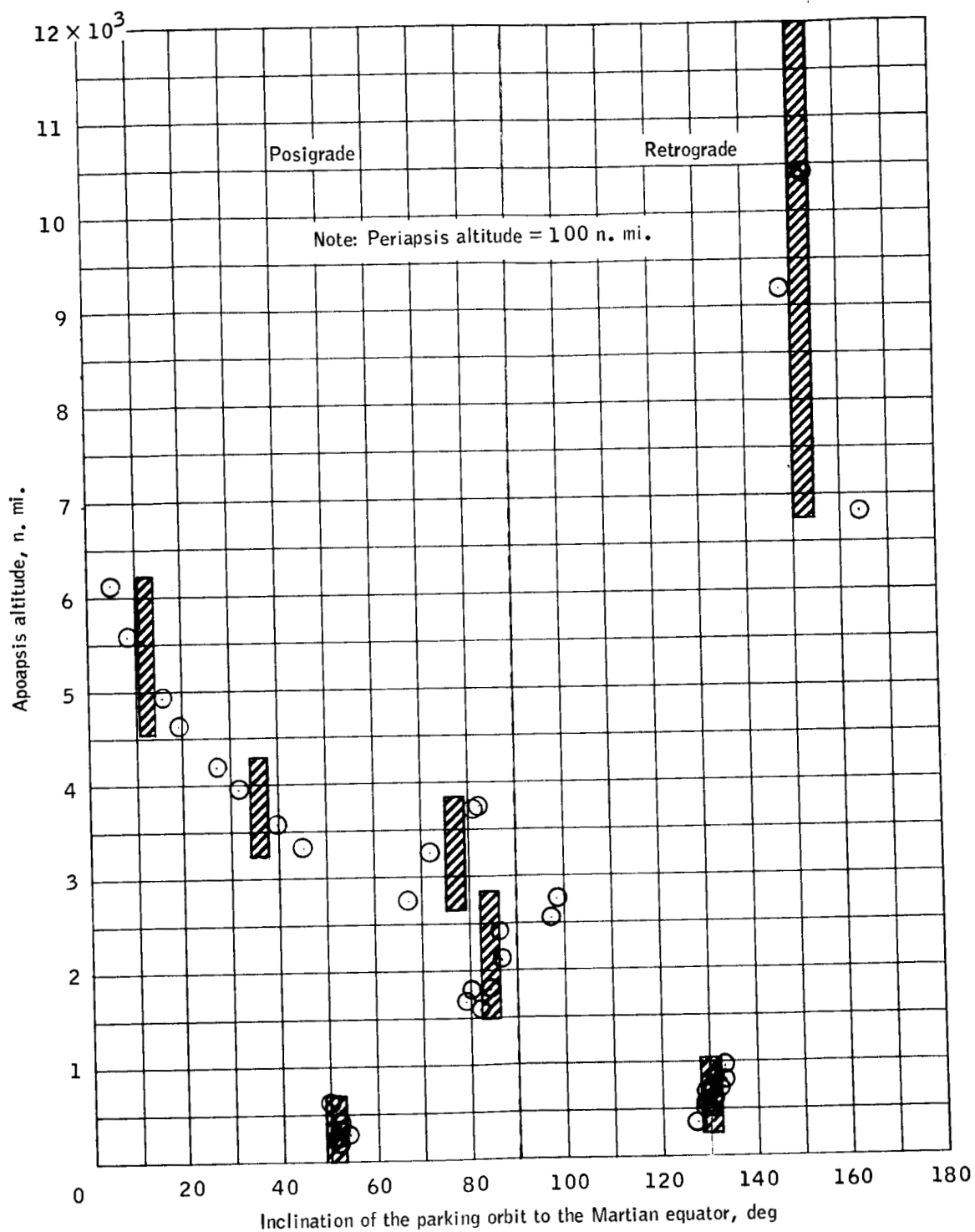


Figure 17.-The correlation of apoapsis altitude and orbital inclination for the short stay time mission in 1986.

REFERENCES

1. Bird, J. D.; Thomas, D. F.; and Collins, R. L.: An Investigation of a Manned Mission to Mars - Trajectories and Mission Analysis. (Paper presented at the Manned Planetary Mission Technology Conference, Lewis Research Center, Cleveland, Ohio, May 21-23, 1963.) NASA TM X-50122, 1963.
2. Bird, J. D.; and Thomas, D. F.: Orbital Rendezvous Considerations for a Mars Mission. Advanced in the Astronautical Sciences, Volume 16, part 1, page 219, (paper presented at AAS Symposium).
3. Thibodeau, Joseph R. III: Use of Planetary Oblateness for Parking Orbiter Alinement. NASA TN D-4657, July 1968.
4. Funk, J.; Taylor, J. J.; Thibodeau, J. R.; Lowes, F. B.; McNeely, J. T.: Manned Exploration of Mars: A Minimum-Energy Mission Plan for Maximum Scientific Return. MSC IN 68-FM-70, April 1, 1968.
5. Henry, E. W.: Trajectory Analysis of Minimum Sum V Mission Plans for Three-Impulse Round-Trip Mars Orbital Missions with Various Fixed-Time Operational Constraints. MSC internal note to be published.
6. Computer Program Documentation Program E181. Conic Interplanetary Mission Planning Program.
7. Bond, Victor R.: Matched-Conic Solutions to Round-Trip Interplanetary Problems that Insure State Vector Continuity at all Boundaries. MSC IN 68-FM-64, March 8, 1968.
8. Bond, Victor R.; and Henry, Ellis W.: One-Way and Flyby Interplanetary Trajectory Approximations Using Matched Conic Techniques. MSC IN 67-FM-16, February 3, 1967.
9. Melbourne, W. G.: Constants and Related Information for Astrodynamical Calculations, 1968. JPL Technical Report 32-1306, July 15, 1968.